THE OPTIMIZATION OF WELL SPACING IN A COALBED METHANE RESERVOIR

A Thesis

by

PAHALA DOMINICUS SINURAT

Submitted to the Office of Graduate Studies of
Texas A&M University
in partial fulfillment of the requirements for the degree of

MASTER OF SCIENCE

December 2010

Major Subject: Petroleum Engineering

THE OPTIMIZATION OF WELL SPACING IN A COALBED METHANE RESERVOIR

A Thesis

by

PAHALA DOMINICUS SINURAT

Submitted to the Office of Graduate Studies of
Texas A&M University
in partial fulfillment of the requirements for the degree of

MASTER OF SCIENCE

Approved by:

Chair of Committee,	Robert A. Wattenbarger
Committee Members,	Bryan Maggard
	Yuefeng Sun
Head of Department,	Stephen Holditch

December 2010

Major Subject: Petroleum Engineering

ABSTRACT

The Optimization of Well Spacing in a Coalbed Methane Reservoir. (December 2010)

Pahala Dominicus Sinurat, B.S., Institut Teknologi Bandung, Indonesia

Chair of Advisory Committee: Dr. Robert A. Wattenbarger

Numerical reservoir simulation has been used to describe mechanism of methane gas desorption process, diffusion process, and fluid flow in a coalbed methane reservoir. The reservoir simulation model reflects the response of a reservoir system and the relationship among coalbed methane reservoir properties, operation procedures, and gas production. This work presents a procedure to select the optimum well spacing scenario by using a reservoir simulation.

This work uses a two-phase compositional simulator with a dual porosity model to investigate well-spacing effects on coalbed methane production performance and methane recovery. Because of reservoir parameters uncertainty, a sensitivity and parametric study are required to investigate the effects of parameter variability on coalbed methane reservoir production performance and methane recovery. This thesis includes a reservoir parameter screening procedures based on a sensitivity and parametric study. Considering the tremendous amounts of simulation runs required, this work uses a regression analysis to replace the numerical simulation model for each well-spacing scenario. A Monte Carlo simulation has been applied to present the probability function.

Incorporated with the Monte Carlo simulation approach, this thesis proposes a well-spacing study procedure to determine the optimum coalbed methane development scenario. The study workflow is applied in a North America basin resulting in distinct Net Present Value predictions between each well-spacing design and an optimum range of well-spacing for a particular basin area.

DEDICATION

This work is dedicated to

My lovely wife, Nova Kristianawatie, for her unconditional love and support

ACKNOWLEDGEMENTS

First of all, I would like to thank the Almighty God for His grace in my life and for showing me the true face of love around me.

I owe immeasurable gratitude to Dr. Robert A. Wattenbarger, for all his kindness. It is truly an honor to be one of his students. I am eternally grateful to him. I would like to acknowledge the suggestions and contributions of my thesis committee members, Dr. Bryan Maggard and Dr. Yuefeng Sun. My gratitude is also due to Dr. William Bryant for his generous help by participating in my thesis defense.

I wish to acknowledge the eternal supports of my parents, wife, brother, and sister.

TABLE OF CONTENTS

CHAPTER Page

Page

LIST OF TABLES

LIST OF FIGURES

FIGURE Page

CHAPTER I

INTRODUCTION

1.1 Background

World energy consumption nowadays is still heavily reliant on fossil fuel to meet basic human needs. Projections of world energy consumption in the future are shown in Fig. 1.1. Currently, the primary energy consumptions in United States are those using coal, nuclear, natural gas, petroleum liquid, biofuel, and also renewable energy (e.g. wind, solar, and geothermal energy). The energy consumption in United States is expected to increase as much as 14 percent from 2008 to 2035. Naturally, it is to be anticipated that the natural gas demand will increase from 23.3 TCF/year in 2008 to 24.9 TCF/year in 2035.

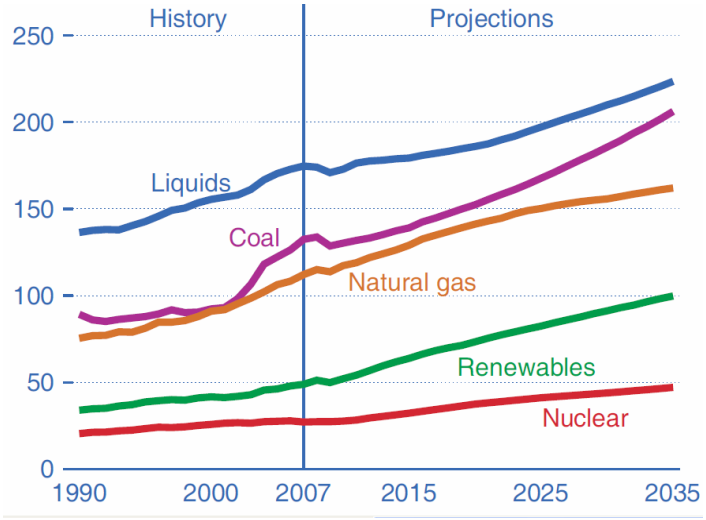

Fig. 1.1 – World energy consumption by fuel type, 1990-2035 (quadrillion Btu)[1]

This thesis follows the style of *SPE Journal*.

To meet the demand, natural gas production needs to be intensified from 20.6 TCF/year in 2008 to 23.3 TCF/year in 2035[2]. The unconventional gas reservoirs (tight gas, shale gas and coalbed methane) have evolved into important sources for the total natural gas production in United States, and, therefore, will also be dominating the natural gas sources by 2035 (Fig. 1.2).

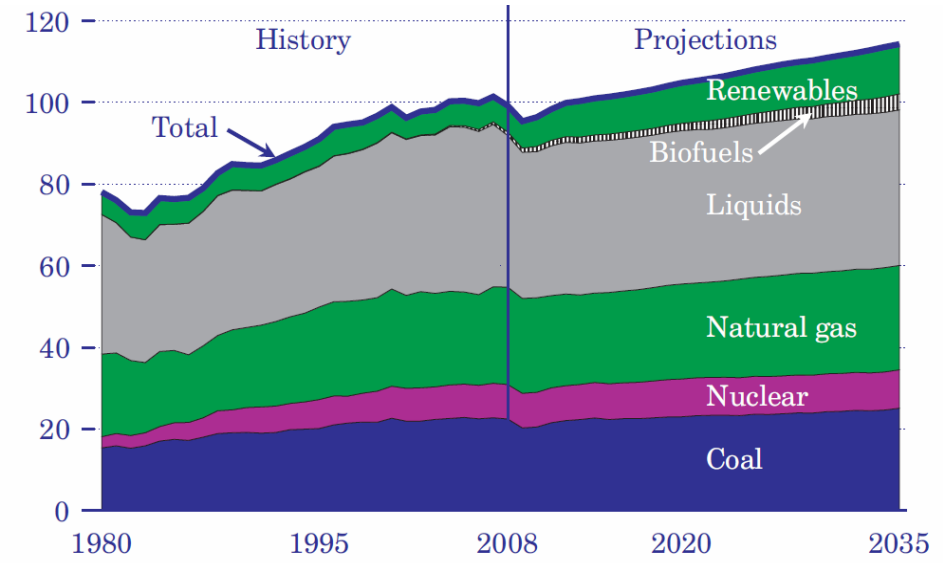

Fig. 1.2 – Energy consumption in US, 1980-2035 (quadrillion Btu)[2]

Unconventional gas reservoirs have contributed a significant amount of gas production in United States. These unconventional reservoirs, such as tight gas, shale gas and coalbed methane in terms of reservoir occurrence, are different from the conventional reservoirs (e.g. sandstone, carbonate). One of its distinctions is that the source rock of unconventional reservoir also acts as reservoir rock[3]. Another explanation of unconventional reservoirs is the application of production technology enhancement such as massive hydraulic fracturing in tight gas, horizontal well and multiple hydraulic

fracturing in shale gas, and steam injection in heavy oil reservoir. The point of such practice is to achieve reservoir production at an economical flow rate at which it will not be so economical to use the conventional production method[4]. Another distinction is its occurrence. In some cases it is also referred to as a basin-centered continuous accumulation where the hydrocarbon distribution is found in a large area. However, it is very difficult to determine the water oil contact in an unconventional reservoir and it tends to be abnormally pressured[5].

Initially, coalbed methane came up as a safety issue in coal mining industry[6]. To minimize risks caused by gas existence, a gas releasing mechanism was taken as an operating procedure in coal mining industry. To produce gas before underground mining operation is commenced, the mining operation utilized a well that was placed in the coal seam.

The United States government's policy then encouraged early unconventional gas development including a coalbed methane reservoir. For instance, the Section 29 tax credit[3] that was initiated in 1980 and took place until 2002 has evoked investments in early coalbed methane development. The tax credit improved the economic value of coalbed methane development by implementing a subsidy of US$ 3 for each barrel (oil equivalent). On the other side, the gas price increment since 1970 also actuated the early coalbed methane reservoir development. A prediction of coalbed methane reservoir contribution on natural gas supply in US is shown in Fig. 1.3.

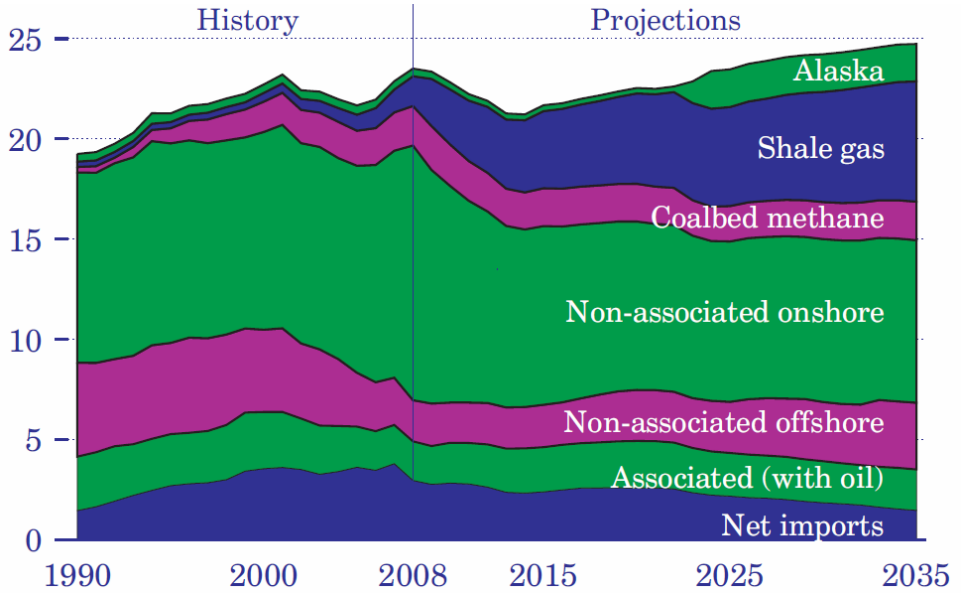

Fig. 1.3 – Natural gas supply in US, 1990-2035 (trillion cubic feet)[2]

Gas in a coalbed methane reservoir is generated during coalification[3] (a process of coal formation from organic matures). During a coalification process, methane, carbon monoxide, and other gases are produced and accumulated on the surfaces area of the internal coal micropores system. The coal seam has the ability to adsorb methane for a large quantity to have an economic value to be produced.

Based on gas generation mechanism, a coalbed methane reservoir is classified as thermogenic and biogenic[3]. Gas generation by a thermogenic process is governed by temperature effects during an organic matter transformation. On the other side, gas generation by a biogenic process is a result of a microorganism activity during a coalification process. Microorganisms transported by water are the source of organic matters during the transformation process.

One advantage of coal as reservoir rock is its capacity to store gas on the internal surface area of coal matrix. The ability of coal to store gas is much higher than a conventional reservoir at an equal rock volume due to extensive surface in the micropores of a coal matrix. Because of its characteristic of storing a larger amount of gas in the adsorption state, coalbed methane has become attractive to be produced by drilling well into the coal seam. A greater storage potential of a coal seam is achieved by higher reservoir pressure. A higher reservoir pressure provides more capacity of coal seam to hold the gas in the adsorption state on the surface area of internal micropores system inside the coal seams. The sorption capacity of coal seam varies based on several factors, such as rank of the coal, coal composition, micropores structure, reservoir pressure, molecular properties of gas adsorbed on the internal surface of coal seam, and reservoir temperature[3,7].

An idealized model of coalbed methane reservoir consists of a matrix system and a fracture system. A matrix system represents the storage of gas inside the coal seam and a fracture system represents the fluid flow path in the coal seam. The behavior of adsorbed gas inside the micropores is modeled by gas inside the matrix system. The mechanics of fluid flow in the coalbed methane reservoir are governed by a cleat system, a natural fracture developed during coalification. The cleat system consists of face cleats network and the butt cleat network. Both natural fracture systems are interconnected and act as fluid flow media outside the matrix system that deliver gas that has been released from the matrix system to the production well. The gas released form the matrix system is strongly related to pressure distribution inside the matrix system. Therefore, the

releasing mechanism of all the gas adsorbed inside the matrix system on the internal surface area depends on the pressure at any time. Since a coalbed methane reservoir modeling concept consists of matrix and fracture systems, the existing dual porosity model concept is commonly applied in the coalbed methane reservoir modeling. However, the fluid flow fundamentals in a matrix system of coalbed methane reservoir is not governed by a potential gradient (Darcy's law), it is more common to model fluid flow inside a coalbed methane matrix system by a gas concentration gradient (Fick's law).

A mathematical model of a dual porosity system that is commonly applied in the oil and gas industry is presented by Warren and Root[8]. The dual porosity model represents fluid flow performance inside two different medias; the matrix and fracture systems. With some modifications, the Warren and Root mathematical model has also been adapted in unconventional gas reservoir, including the coalbed methane reservoir.

The main fluid flow path in the coalbed methane reservoir is the cleat system. An idealized model of a cleat system in the coalbed methane reservoir as presented in Fig. 1.4 consists of the face cleats system and the butt cleats system. In the coal natural fracture system, the fracture density depends on the thickness and ash content. Greater fracture density occurs more commonly in thin coal than in thick coal. Ash content in coal seam also influences the fracture density, bulk density and coal rank[7]. The stress distribution available in the field during a coalification process influences the generated fracture direction. The direction of continuous cleat or face cleat in the coal seam is governed by stress orientation. Face cleat orientation tends to be perpendicular to the

minimum stress direction. Permeability anisotropy in the coalbed methane reservoir is related to the developed cleat system.

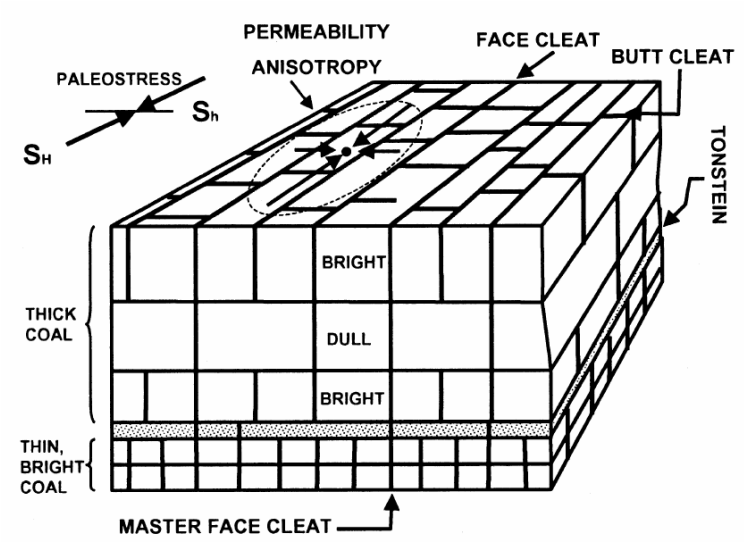

Fig. 1.4 – Schematic cleat characteristics[3]

Methane production from a coal matrix can be achieved by lowering the reservoir pressure or the partial pressure of adsorbed gas in a coal matrix. Gas desorption occurs after the pressure declines until it reaches below the desorption pressure. Therefore, coalbed methane production methods depend on how to reduce overall pressure within the reservoir body by producing the formation water.

Water treatment technology in a coalbed methane operation was developed by modifying conventional gas production facility. For instance, a separator design in coalbed methane operation is prepared for formation water handling and separation of solid content from coal mines. The main difference of water production characteristics in

coalbed methane is that it has a lower total of dissolved solids or in other words, it is fresher than the conventional gas water production.

As water is produced from the wellbore, the pressure reduction starts to occur around the wellbore. Pressure reduction disperses through a reservoir body until the hydrostatic pressure reaches below the adsorption pressure, and at this condition methane gas desorption starts to take place. After desorption occurs, methane gas starts to migrate through permeable strata, especially the cleat system to the lower pressure area toward the wellbore area. In the near-surface area, coal outcrops may experience hydrostatic pressure reduction followed by desorption and gas migration through porous media to the surface or are entrapped with groundwater.

Different with conventional gas production characteristics, coal bed methane reservoir production performance has a unique production trend. At the beginning, when the reservoir pressure is higher than the desorption pressure, no gas will be produced. After the reservoir pressure declines and falls below desorption the pressure by producing formation water, then gas starts to desorb. During this initial stage, the gas production will increase until it achieves its peak production. After such peak production, the production performance will be similar with the conventional gas production. Conventional gas reservoir gas production behavior is related with pressure-depletion in the reservoir, so after peak production it will decline until it does not have any pressure or production pressure constraint. While the desorption process in a coalbed methane reservoir is governed by pressure reduction in the reservoir, the driving mechanism of gas methane flow in the cleat system is influenced by the difference of the

reservoir pressure and the wellbore pressure. The energy of a gas methane flow is derived from the reservoir pressure. On the other side, the reservoir pressure reduction helps gas methane to desorb from the matrix surface area. Coalbed methane reservoir production strategy through pressure depletion is quite common in the industry and about 50 percent of gas in place could be economically recovered by implementing the depletion strategy[9].

Gas in a coalbed methane reservoir is stored by adsorption mechanism. The gas is attached on the internal surface area of the coal matrix. After the reservoir pressure declines until it reaches below desorption pressure, gas starts to desorb from the internal surface area of the coal matrix. The gas drainage mechanism may be explained better by molecular diffusion (Fick's law) rather than the fluid flow derived from the pressure difference (Darcy's law). The process of gas drainage according to the diffusion process is related with sorption time. Sorption time is a value that represents a characteristic of a drainage process which is the required time to desorb methane gas for a constant pressure and temperature condition. A typical production performance of a coalbed methane reservoir is presented in Fig. 1.5.

As shown in Fig. 1.5., the first stage of production profile is the dewatering process. The dewatering process is a mandatory procedure in a coalbed methane reservoir with higher reservoir pressure than the desorption pressure. Therefore, during the initial production stage, the only fluid produced from the wellbore is formation water. The fundamental of a fluid flow in this initial stage is exactly similar with conventional gas reservoir, the water flows through the cleat system or any permeable

strata governed by Darcy's law. Since water production has been initiated, reservoir pressures start to decline. After the declining pressure reaches the desorption pressure, methane gas starts to desorb.

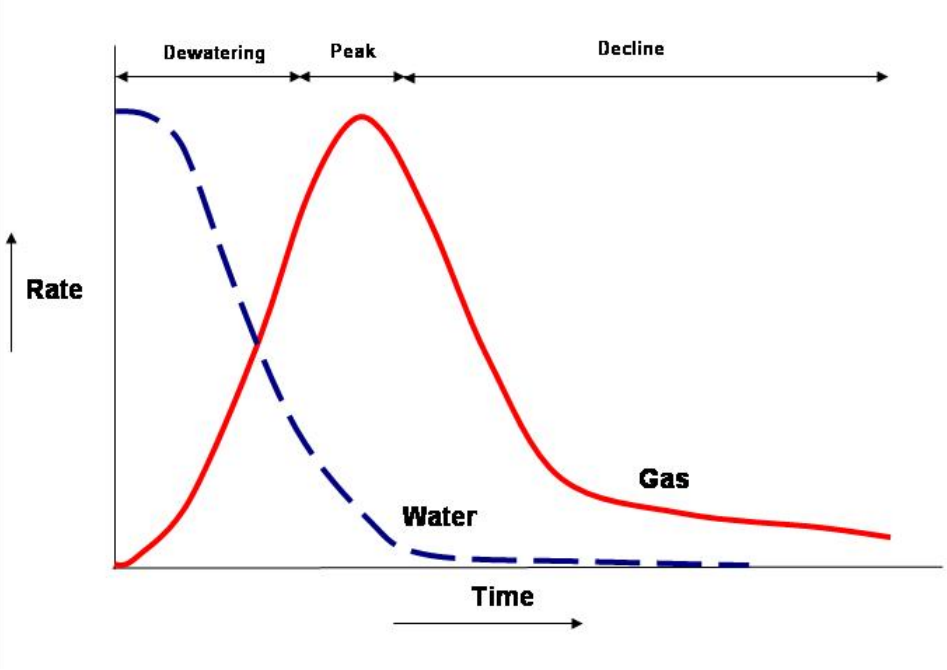

Fig. 1.5 – Typical coalbed methane production behavior

As shown in Fig. 1.5., the first stage of production profile is the dewatering process. The dewatering process is a mandatory procedure in a coalbed methane reservoir with higher reservoir pressure than the desorption pressure. Therefore, during the initial production stage, the only fluid produced from the wellbore is formation water. The fundamental of a fluid flow in this initial stage is exactly similar with conventional gas reservoir, the water flows through the cleat system or any permeable strata governed by Darcy's law. Since water production has been initiated, reservoir

pressures start to decline. After the declining pressure reaches the desorption pressure, methane gas starts to desorb.

The gas resulted from desorption process causes a concentration gradient within the matrix system. At this stage, Fick's law is more appropriate to be used as a fundamental equation of gas methane drainage phenomenon. Because reservoir fluid has been recovered, the reservoir pressure declines and water production will also decrease. As the water production decreases caused by lower reservoir pressure, gas production increases resulting from the desorption process.

The gas rate will keep increasing until it achieves peak production. In this early time, the gas production behavior is strongly related to the diffusion process. Eventually, after reservoir pressure depletion becomes a more significant factor, the gas production behavior will follow Darcy's law. Therefore, gas starts to decline and the production performance will be governed by the pressure gradient. Pressure reduction will also influence permeability and porosity because a coal matrix tends to shrink at a lower pressure condition. In this case, the porosity value will be lower and it will change the reservoir permeability as well.

The gas production profile is different in the dry coal system. In this system, the initial formation water does not exist in the reservoir. Therefore, gas production occurs from the early well life and a dewatering process is no longer required. The production profile is almost similar with a conventional gas reservoir. However, a desorption process is still an important mechanism of the depletion strategy. One should consider a desorption process after the reservoir pressure reaches a lower value than the desorption

pressure. At this stage, gas desorbs from the internal surface of the coal matrix and gas drainage within the coal matrix starts to take place due to the gas concentration difference (diffusion process). Afterward, gas starts to flow through the permeable strata and the cleat system into the welbore. There are several papers available explaining the production performance behavior in a coalbed methane reservoir considering the complex relationships among adsorption, diffusion, and matrix shrinkage along the reservoir life cycle.

1.2 Problem Description

In coalbed methane reservoir development plan, well spacing scenario is an important issue to estimate overall project feasibility. In the other side, there are several uncertainties in reservoir properties that should be taken into account during the decision making process. The uncertainties include the coal density, permeability or gas content as parameters of coal properties. Each coalbed methane reservoir property will govern production performance in a certain degree. Some parameters strongly influence production behavior, for instance coal matrix gas content or coal system effective permeability. However there are also other parameters with less contribution than the others on the alteration of overall gas production performance.

Economic calculation of each well spacing scenario depends on the prediction of future production performance. Instead of randomly considering variation of possible parameters, it is often necessary to perform a sensitivity analysis and parametric study to

select the most influential factors in the reservoir model that will determine future production performance.

1.3 Objectives

This work intends to investigate the effects of coalbed methane reservoir properties to reservoir development scenario especially the well spacing strategy. Coalbed methane reservoir production performance is modeled by a reservoir simulation. A reservoir simulator will be utilized to investigate and document the effects of coalbed methane reservoir properties on the selection of well spacing scenario. A parametric study and sensitivity analysis are performed on numerous combinations of reservoir parameters. A screening procedure is also provided to guide parameters selection in the sensitivity analysis and parametric study process. The effect of each parameter variation is investigated to determine the influence of parameter uncertainty to the gas flow behavior in the coalbed methane reservoir simulation model.

1.4 Organization of this Thesis

The study is divided into five chapters. The outline and the organization of this thesis are as follows:

Chapter I presents an overview of coalbed methane reservoir. The research problem is also described in this chapter as well as the project objectives.

Chapter II presents a literature review. This chapter gives the existing overview about coalbed methane reservoir occurrence and development, fundamentals of the fluid

flow in a coalbed methane reservoir, coalbed methane reservoir modeling, and economic modeling.

Chapter III presents fundamentals of coalbed methane reservoir engineering and sensitivity study. The reservoir engineering approaches include gas storage mechanism, the fluid flow in a coalbed methane reservoir, and the reservoir simulation. This chapter also provides fundamentals of a sensitivity analysis and Monte Carlo simulation.

Chapter IV presents simulation results on a specific data set, the sensitivity study, and an economic model. The evaluation includes well spacing effects. This chapter gives insights about the decision making procedure, especially well spacing determination.

Chapter V presents the conclusions and future recommendations.

CHAPTER II

LITERATURE REVIEW

2.1 Introduction

It is common to consider a coalbed methane reservoir as a dual porosity or naturally fractured reservoir. A coalbed methane reservoir is a naturally fractured reservoir with a coal matrix that has the potency as methane gas storage. Storage mechanism in a coalbed methane reservoir could be explained by an adsorption process. An adsorption process enables gas to be attached on the internal surface area of the coal matrix. On the contrary, with a desorption process, methane gas is released and gas drainage occurs, which allows gas to be transported through permeable media or a fracture system. A fracture system in the coalbed methane reservoir is strongly related with the cleat system. The fracture system, in this case the face cleat and butt cleat, acts as a porous medium and cause reservoir anisotropy. The face cleat is more continuous and longer than the butt cleat, and it tends to exist continuously through the reservoir body. On the other side, the butt cleat is a perpendicular fracture that is shorter and discontinuous. The butt cleat is discontinuous because during natural fracture formation it is intersected by face cleats. Face cleats tend to be more continuous because they are first-formed fractures and are more systematic. The butt cleat is a secondary natural fracture system and is less systematic during its development than the face cleats, so this natural fracture system contributes to the reservoir anisotropy. The face cleats also provide a larger interface area with the matrix system than the butt cleats do. This

phenomenon makes the face cleats more important in the fluid flow mechanism. It is common to assume the face cleat direction as the maximum permeability direction. However in some cases, this is not a correct assumption, such as in the case of Bowen basin, Australia[11].

The storage capacity of a coal matrix can be considered as a economic resource; however the coal matrix permeability is very low. The coal fracture system, particularly the cleat system, provides media for fluid flow in the coal system. The cleat system contributes to overall formation permeability. Methane gas resulting from desorption process flows through the cleat system or natural fractures into the wellbore. The permeability anisotropy is related to the formation of face cleats and butt cleats, in this case the anisotropy creates a preferential flow. It is more common to find the maximum permeability orientation parallel with the face cleat direction. Furthermore, the drainage pattern will also be determined by permeability anisotropy.

2.2 Dual Porosity Model

The first dual porosity model was introduced by Barenblatt, G.I., Zheltov, I.P., and Kochina, I.N.[10]. A further development of a dual porosity model was then presented by Warren and Root[8], who proposed the application of a dual porosity model in well testing interpretation. The Warren and Root dual porosity model later became a basic concept in the development of naturally-fractured reservoir characterization techniques. Most unconventional reservoirs for gas such as tight gas, shale gas, and coalbed methane are classified as naturally-fractured reservoirs. As shown in Fig. 2.1, Warren and Root

proposed a conceptual model for a naturally-fractured reservoir by modeling a homogeneous matrix block that is separated by fractures. The matrix block serves as storage for adsorbed gas and the fracture system provides media for the fluid flow within the reservoir body, from the matrix to the fracture system, which is followed by the fluid flow from the matrix system to the wellbore. The overall formation permeability is strongly related with a fracture or cleat system.

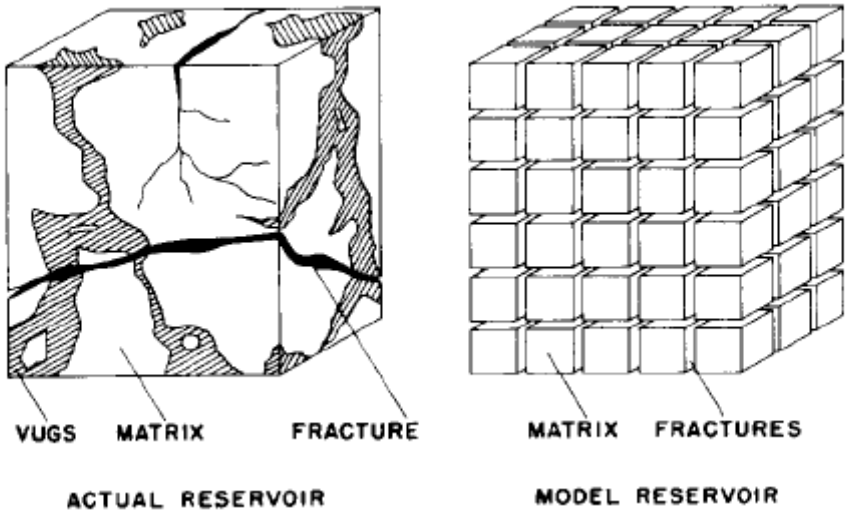

Fig. 2.1 – Schematic of dual porosity model[8]

The dual porosity concept proposed by Warren and Root is also applicable in a coalbed methane reservoir. The dual porosity concept provides an idealized model of reservoir performance in two different types of media. The first medium is storage that contributes to the pore volume but with very low flow capacity. The second medium is a fracture system which contributes to fluid flow. Warren and Root classified porosity into

two categories. The first one is the primary porosity controlled by deposition and lithification. The second type of porosity is the secondary porosity; a porosity that is controlled by water solution, natural fracturing, and jointing. A mathematical model for this description is presented for the application of a pressure build-up analysis. The idealized model is derived at an unsteady state condition and presented with two additional parameters to characterize the dual porosity system. The two additional parameters are ω and λ. The first parameter, ω, serves as a model fluid capacitance. This parameter is introduced as storativity, a measure of fracture system storage capacity. The second parameter, λ, refers to the heterogeneity exists in the dual porosity system. This parameter is introduced as an interporosity flow parameter or flow capacity. The mathematical model presented by Warren and Root is derived at a pseudosteadystate condition (semisteadystate or quasistedystate). An equation for this interporosity flow from the matrix system to the fracture system in a mathematical point is presented as

$$q = \sigma \frac{k_m}{\mu}\left(p_m - p_f\right)$$

An application of the mathematical model was prepared for pressure buildup analysis. Pressure buildup data show parallel lines on a semilog plot. The parallel lines are separated by a transition with S-shaped. The first line represents the fluid flow in the fracture system. After the transition period occurs, the second line appears as a representation of the total system behavior (both of matrix and fracture system).

2.3 Coalbed Methane Reservoir Modeling

Previous studies have investigated the effect of coalbed methane properties variance on the production performance. David, Turgay, Wonmo and Gregory[11] presented a mathematical model to simulate methane and water flows through the coal seam and the effect of coalbed methane reservoir properties on gas drainage. This work uses single and multiple well systems. Olufemi, Turgai, Duane, Grant, Neal *et al.*[12] conducted numerical reservoir simulations to study the effects of coal seam properties variability in an enhanced coalbed methane project. They used a numerical simulation model to show the most influential parameters that affect recovery in an enhanced coalbed methane reservoir project. However, most of these works did not cover the development of fundamentals of the fluid flow and adsorption-desorption phenomenon in numerical modeling.

Cervik[13], in 1967, presented a basic concept of transport phenomenon for gas at a free gas and desorption state. This work showed gas dependency of gas desorption phenomenon to the coal particle size, equilibrated pressure and diffusivity coefficient. It showed that smaller particle tends to provide more gas. He proposed three classifications of gas transport phenomena. The first one was principally Fick's law while the second one was a combination of Fick's and Darcy's law, and the third one was predominantly Darcy's law. Base on the results, it was not recommended to use the same basic concept for conventional gas reservoir engineering in a coalbed methane reservoir model, since the Darcy's law and Fick's law govern overall mass transport phenomenon.

By using a numerical simulator, Zuber, M.D., Sawyer, W.K., Schraufnagel, R.A., and Kuuskaraa, V.A.[14] illustrated the procedure to determine coalbed methane reservoir properties by using a history-matching analysis. The numerical simulator was modified to adjust the flow and storage mechanism in a coalbed methane reservoir. In the history-matching process, a two-phase dual porosity simulator was used to model reservoir performance based on production data, geological data, and laboratory data.

Another work conducted by Seidle[15] presented a methodology to utilize a conventional reservoir simulator with some input data modification to model a coalbed methane reservoir. This work assumed an instantaneous desorption that occurred from the matrix block to the cleat system by using the analogy of dissolved gas in immobile oil for a conventional reservoir simulator as adsorption gas on the internal surface of a coal matrix. This work showed that the rate of diffusion in the matrix system was much higher than the fluid flow in the cleat system. Therefore, this work analogizes gas adsorption as saturated gas in immobile oil. In this case, the solution gas oil ratio is determined by the Langmuir isotherm equation.

Fig. 2.2 shows the correlation between gas content and pressure. A modification relative permeability curve is proposed to account the pseudo oil. The modification of input data is applied on porosity and relative permeability curves (gas-water systems) considering the existence of the immobile oil. However, this work did not modify basic equation in the simulator. The works were verified by comparing a commercial simulator for black oil with a coalbed methane reservoir simulator.

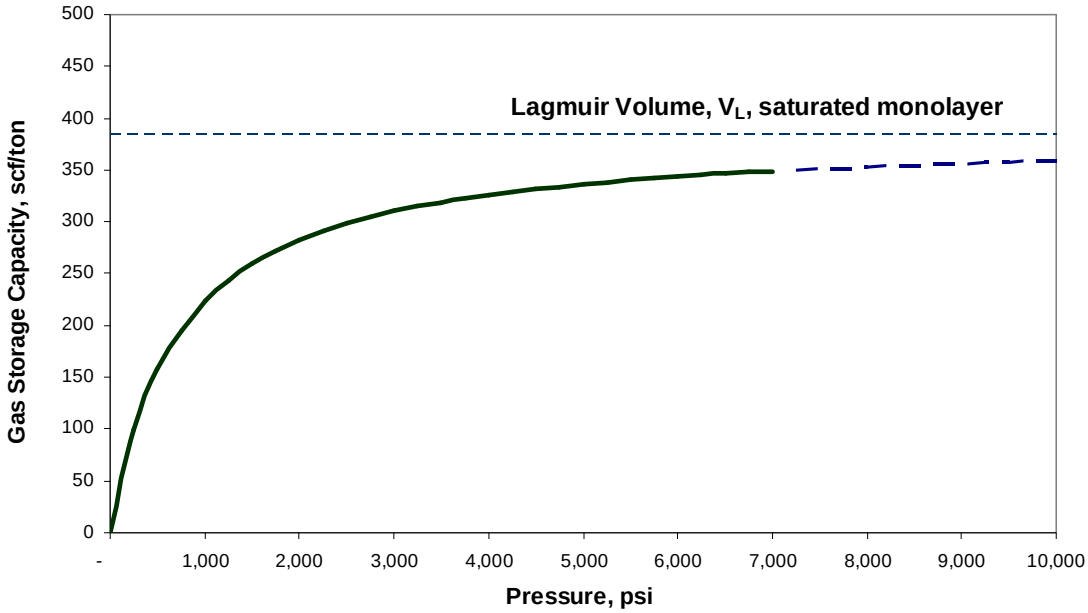

Fig. 2.2 – Langmuir isotherm curve

Another work on conventional gas reservoir engineering adapted to coalbed methane reservoir was presented by King[16]. His work showed a modification of material balance concept for reserve estimation and prediction of future production performance in unconventional gas reservoirs. This work utilized fundamentals of conventional gas reservoir engineering for material balance techniques in a coalbed methane reservoir with the effects of gas desorption and diffusion in consideration. The material balance analysis assumed an equilibrium state of gas and adsorbed gas in the coal system. A pseudo-steady state condition was also assumed to be applied during the sorption process. This work provided a procedure of gas in place estimation by using the p/z method and prediction of future production performance based on the existing material balance techniques.

A modification of King's method was presented by Seidle[17] with more advanced techniques in material balance. His work provided fundamentals of a mathematical model, simulation studies, and examples of field application. The modified method improved material balance techniques by eliminating mathematical problems and suggesting more accurate reserve estimation for a coalbed methane reservoir.

Other numerical reservoir simulation studies were presented by David, H. and Law, S.[18], Hower, T.L.[19], and Jalal, J. and Shahab, D.M.[20]. They showed the application of a compositional simulator in coalbed methane reservoir modeling. The numerical compositional simulator was equipped with some additional features for coalbed methane reservoir modeling. David and Law's work showed coalbed methane enhanced the recovery model by using a compositional numerical simulator. The enhanced recovery method is the CO_2 injection. The compositional simulator was able to model more than two components. This work assumed instantaneous process of gas diffusion from the matrix system to the fracture system.

Aminian, K., Ameri, S., Bhavsar, A., Sanchez, M., and Garcia, A.[21] presented another approach of predicting coalbed methane gas production performance by using a type curve matching based on gas and water rates. This method used dimensionless rate and time. It also showed the application of the type curve matching for determining the matrix and cleat porosity based on production- history matching. Based on the matching results, future production performance could be estimated to evaluate the coalbed methane reservoir prospect. This study also provided a correlation of the peak gas rate to predict future production performance.

A later work by Reeves, S. and Pekot, L.[22] presented a mathematical model for a desorption-controlled reservoir. They introduced the model as a triple-porosity dual-permeability model. This mathematical model was a modification of Warren and Root's model. This work showed the erroneous result of the previously existing dual-porosity single-permeability model in predicting coalbed methane reservoir performance. An overestimation of gas and water production tended to appear with the inconsistency of the model result and field data. In fact, gas production was found much higher than the gas predicted form the model in later time. To model this phenomenon, a set of porosity and permeability was added to the system. The third porosity was introduced in the matrix block system to provide free gas and water storage capacity for the modification of material balance techniques. This work also provided decoupled models of a desorption process from a matrix block and the diffusion process through a micro-permeability matrix so that mass transport could be explicitly determined. A comparison of the existing model result and the proposed model result was shown with a higher water rate and lower gas rate which were more accurate and matched with field data. This work also introduced a new coalbed methane simulator, COMET2 with some modifications in the fundamentals of the fluid flow and desorption process.

A modification of Seidle[15] approach was presented by Thomas, Tan.[23], in 2002. His work also used a commercial simulator to model coalbed methane reservoir performance with independent implementation. He also showed a comparison of his result in a paper by Paul, G.W., Sawyer, W.K,. and Dean, R.H.[24]. This work illustrated pressure dependent porosity and permeability phenomenon with some comparative runs.

The result was not consistent with Seidle' paper, but, as reported, it was an excellent match for Paul's paper. Tan's work also suggested the dual grid approach to gain a more accurate result in a matrix-fracture model.

In 2003, Xiao Guo, Zhimin Du, and Shilun Li[25] presented a more sophisticated numerical simulator with 3 dimensional and two-phase flow calculation capability. The new simulator improved coalbed methane reservoir characterization by including transport phenomena in the coal micropores and fracture system. The gas resulting from the desorption process was calculated with a sorption isotherm curve from the experiments and calculation. Therefore, an equilibrium state of desorption process was necessary to be considered.

2.4 Coalbed Methane Reservoir Sensitivity Study

David, Turgay, Wonmo and Gregory[11] investigated the relationship between the peak gas rate and the ability of a matrix system to desorb gas. They performed a sensitivity study to observe the consistency of new reservoir simulator results. The study included an investigation of absolute permeability, sorption time for the gas diffusion rate, and relative permeability effects on methane recovery for various well spacing scenarios. The sensitivity study incorporated the effects of reservoir property variation on the drainage efficiency of gas in the coal matrix system. This work used a single well model.

Another work by Olufemi, Turgai, Duane, Grant, Neal, et al[12] investigated the effect of coalbed methane reservoir properties on production performance in a enhanced

coalbed methane project. A reservoir simulator was used to model reservoir performance and select most influential parameters affecting gas recovery. It showed that reservoir permeability, coal density, and Langmuir volume were the most significant factors in methane recovery of a CO_2 sequestration study.

Derickson, J.P., Horne, J.S., Fisher, R.D., and Stevens, S.H.[26] presented a sensitivity study result for coalbed methane reservoir production performance in Huaibei, China. This work investigated the effects of some fundamental coal properties variation on the production rate. They concluded that coal permeability, gas content, initial water saturation, and coal thickness were the most influential factors related to gas production.

Roadifer, R.D., Moore, T.R., Raterman, K.T., Farnan, R.A., and Crabtree, B.J.[27] conducted a comprehensive study with more than 100,000 simulation runs. The study was aimed to perform a parametric study incorporated with a Monte Carlo simulation analysis. Numerous combinations of reservoir properties, geological data, completion and operation constraint were prepared in the simulation runs to investigate the effects on production performance. Relative importance of each parameter and inter-parameter relationship were identified. Rank correlation was developed based on simulation results considering several production constraints, such as the peak gas rate, dewatering times, and cumulative gas production. Core sample acquisition in coal seams was difficult due to its tendency to be extremely friable. This friability complicated the reservoir properties measurement especially for permeability, porosity, compressibility and relative permeability data. This paper explained the differences between a sensitivity

study and a parametric study based on basic concepts. The sensitivity study was performed by changing one value while keeping the other values at the base value. On the other side, a parametric study was conducted by preparing all possible combinations of each parameter at every value (e.g. minimum, most likely, and maximum).

Stevenson, M.D., Pinczewski, W.V., and Downey, R.A.[28] conducted a sensitivity study for a nitrogen-enhanced coalbed methane study. This work investigated the effects of reservoir parameter variation on the project economics based on predicted gas production. The reservoir parameters that were identified as the most significant factors were permeability, relative permeability, compressibility, layering and capillary pressure. For each parameter, the minimum, most likely, and maximum values were taken into account. San Juan basin data were chosen to be used in performing the sensitivity study.

Reeves, S.R. and Decker, A.D.[29] performed a discrete parametric study for a wide range of the reservoir depth, pressure gradient, Langmuir volume, and permeability as a function of pressure and depth. Young, G.B.C., McElhiney, J.E., Paul, G.W., and McBane, R.A.[30] presented a distinct parametric study for San Juan basin area. This work divided San Juan basin into three areas for a discrete parametric study based on reservoir properties variations. For instance, in Area 1 the sensitivity study covered permeability, porosity and drainage variation. In Area 2 permeability, porosity, drainage area and fracture half-length were investigated for a particular range. In Area 3, a sensitivity study was performed for the coal compressibility, gas content, Langmuir parameter and relative permeability ratio.

2.5 Well Spacing Effect

In a coalbed methane reservoir, well interference effect improves the pressure reduction process by dewatering formation fluid from a cleat system. Interference between coalbed methane wells causes the decline of reservoir pressure and helps the initiation of the gas desorption process. Unlike a conventional gas reservoir, well interference in a coalbed methane reservoir is an advantageous condition. David, Turgay, Wonmo, and Gregory[11] performed a parametric study to investigate well interference effect in a coalbed methane reservoir. They used a multiple-well system to observe gas and water production performance related to well interference. This work concluded that interference between coalbed methane wells improved the gas methane desorption process from the matrix to the cleat system by adding the pressure drawdown in the coal matrix system. On the other side, water production performance tended to show similar behavior for well interference effect in a conventional gas reservoir.

Another well-spacing study was conducted by Young, G.B.C., McElhiney, J.E., Paul, G.W., and McBane, R.A.[31] by using a numerical reservoir simulation for Fruitland coals in Northern San Juan Basin. This work showed the increment of methane gas recovery factor in a reservoir model with smaller well-spacing. This work also included fracture half-length as a variable in determining the most optimum development scenario. The optimum well-spacing and fracture half-length depended on coalbed methane reservoir variability. Young, G.B.C., McElhiney, J.E., Paul, G.W., and McBane, R.A.[31] continued their study with an investigation on well spacing effects on the early peak production and gas decline rate. The study showed that the initial peak gas

rate tended to be higher in smaller well-spacing. On the other side, the gas decline rate was higher in a smaller well-spacing scenario.

Another well-spacing study was conducted by Wicks, D.E., Schewerer, F.C., Militzer, M.R., and Zuber, M.D.[32] in Warrior basin coalbed methane reservoir. To investigate the effects of well spacing on methane recovery, they compared production performance of 8 wells in 160 acres with 1 well in the same area. Their study found that smaller well-spacing (8 wells in 160 acres) yielded 85 percent methane gas recovery while 1 well in 160 acres only gave 25 percent methane gas recovery. However, this work did not include economic factors on selecting the most optimum well-spacing scenario.

Chaianansutcharit, T., Her-Yuan Chen and Teufel, L.W.[33] also presented well interference effects in coalbed methane reservoir production performance. They used a numerical simulator to model coalbed methane reservoir performance for various well-spacing scenarios. Their study showed that methane gas recovery tended to be higher in a two-well system than a one-well system. This means that, unlike in a conventional gas reservoir, interference effects would accelerate gas production.

CHAPTER III

COALBED METHANE RESERVOIR MODELING

3.1 Introduction

To characterize a coalbed methane reservoir, a dual porosity reservoir concept can be applied. A coalbed methane reservoir consists of a matrix system and a fracture system. The matrix system basically provides gas storage capacity in the internal surface of coal micropores. During the coalification process, methane gas is adsorbed on the internal surface area of coal. Due to the adsorption phenomena and low pressure system, the fundamentals of characterizing a coalbed methane reservoir are different from that of a conventional gas reservoir.

The fracture system is a conduit of a fluid flow after methane gas is desorbed from coal matrix. A coalbed methane reservoir facture system is categorized into two major natural fracture systems. The longest and a more continuous natural fracture system is the face cleat. The shorter and more discontinuous fracture system is the butt cleat system. The butt cleat system direction is perpendicular to the face cleat direction and therefore intersected by the face cleat system. Since the face cleat contact area to matrix system is larger, the gas drainage process is more prominent in face cleat contact area. Therefore, the face cleats contribute more on the methane gas fluid flow. An example of a coal cleat system is shown in Fig. 3.1.

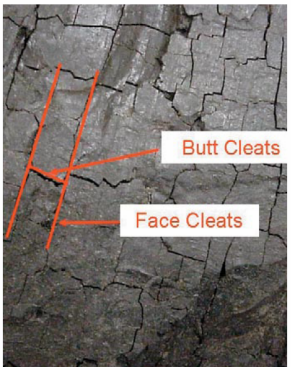

Fig. 3.1 - Structure of coal cleat system[4]

To develop an adequate coalbed methane reservoir model, it is necessary to have understanding about physical properties of a coalbed methane reservoir parameter and its relationship on the desorption mechanism, diffusion process and fluid flow inside the coal cleat system. This chapter will introduce the fundamental theories that govern the coalbed methane reservoir performance behavior.

3.2 Gas Storage in Coalbed Methane Reservoir

The gas storage mechanism in a coalbed methane reservoir is different from the one in a conventional gas reservoir. The methane gas is formed during the coalification process, coal formation from plant material conversion. During the coalification process, methane occurs as a byproduct and is adsorbed into the internal surface of the coal micropore system. Therefore, a coalbed methane reservoir is also considered as both source rock and reservoir rock.

Most of the gas is stored in a coalbed methane reservoir by an adsorption process. The main driving force of an adsorption process is molecular attraction (Van

Der Walls forces). The physical of an adsorption process is governed by intermolecular attraction between gas molecules and solid surfaces of the coal micropore system. Gas methane is also present in a coalbed methane reservoir in several different ways. It can be free gas compressed in the micropores system. Gas can also exist as free gas in the pore system (where the pores are bigger than micropores) and the fracture system. Another way of gas storage is dissolved in formation water.

As free gas, the methane gas is stored in the pore spaces. A normal gas law principle can be applied in this condition; therefore, the amount of free gas can be estimated by knowing the porosity and pressure value. The amount of free methane gas is very small compared the adsorbed gas.

The coalbed methane storage capacity is much higher than that of a conventional gas reservoir at an equivalent pressure and temperature condition. This characteristic makes a coalbed methane reservoir is attractive to be exploited. The internal surface area of the coal matrix micropore system is very large, and, thus, it enables more gas to be stored at adsorption condition. For some coal types, the internal surface area of the micropore system can reach hundreds of square meters per gram of solid[12]. The coal seam capacity to store gas is 6 to 7 times higher than that of sandstone at the same equivalent depth[7].

The coal seam gas storage capacity is a function of pressure within the micropore system. The amount of adsorbed gas is controlled by the free internal surface area of the coal micropore system. The Langmuir adsorption isotherm curve can be used as a function to estimate the adsorbed gas at a given pressure with a constant temperature

condition. The Langmuir adsorption isotherm curve is a reservoir parameter that represents the amount of gas that will be desorbed if the reservoir decreases until it reaches a value below the desorption pressure. Each time the gas is released, the gas concentration at a given point will decrease and there will be an equilibrium state between the pressure and the amount of adsorbed gas. Theoretically, at the zero pressure, all the adsorbed gas will be released from the surfaces area of the internal coal micropores system.

3.3 Gas Transport Mechanism

At the initial condition, most of the methane gas is adsorbed on the internal surface area of the coal matrix micropore system. Generally, the fracture system is only saturated with formation water with negligible soluble gas. Unlike a conventional gas reservoir, only a very small amount of gas is stored as free gas in the pore system.

Therefore, to release adsorbed gas, the pressure inside the coal seams system should be reduced until it reaches a lower value than the desorption pressure. The first stage of coalbed methane production is initiated by producing formation water only. This procedure is often named as a dewatering process. By producing formation water from the cleat system, reservoir pressure will be decreased in proportion to the volume of water removed from the cleat system.

After the matrix pressure system reaches a value lower than the desorption pressure, the adsorbed gas on the internal surface area of the coal matrix micropore system starts to desorb into the cleat system. The volume of released gas follows the

Langmuir isotherm curve and alters gas concentration at a given point. Because of the presence of a gas concentration gradient, the diffusion process from the matrix system to the fracture system begins to occur. Once the released gas enters the natural fracture system, it flows through the cleat system into the wellbore. To summarize, there are three main processes of gas transport phenomena in the coalbed methane reservoir system. The first process is desorption when gas is released from the surfaces area of the internal coal micropores system. Afterwards, the diffusion process takes place. Governed by a concentration gradient, the desorbed gas flows from the coal matrix into the cleats system. Finally, the gas flows through the permeable strata and the cleat system, which is governed by the pressure gradient.

The gas transport phenomenon in a coalbed methane reservoir is measured by two main parameters; the coal permeability and diffusivity. As the reservoir decreases, the adsorbed gas is released from the surfaces area of the internal coal micropores system. The releasing mechanism follows the desorption process. Since the micropore size is very small, the gas is transported at a very slow rate and is governed by the difference of gas concentration. In a very small micropore system, the gas flow rate follows the diffusion rate rather than the fluid flow mechanism explained by Darcy's law. The main reason of this phenomenon is the existence of drag force which is very high in the very small pore throat size. The diffusivity term represents the gas diffusion rate at a given point. The coal permeability determines gas the flow rate through permeable strata or the cleat system.

Fig. 3.2. shows three main processes in the coalbed methane transport phenomena. The matrix is the micropore system while the fracture is the macropore system. The fluid flow in each system follows different mechanisms. The desorption process occurring in coal particles releases methane gas from the internal surface area of the coal matrix. The diffusion process enables gas to be transported through the micropore system. Eventually, fluid flows occur within cleat system which is governed by the pressure gradient of the well being produced.

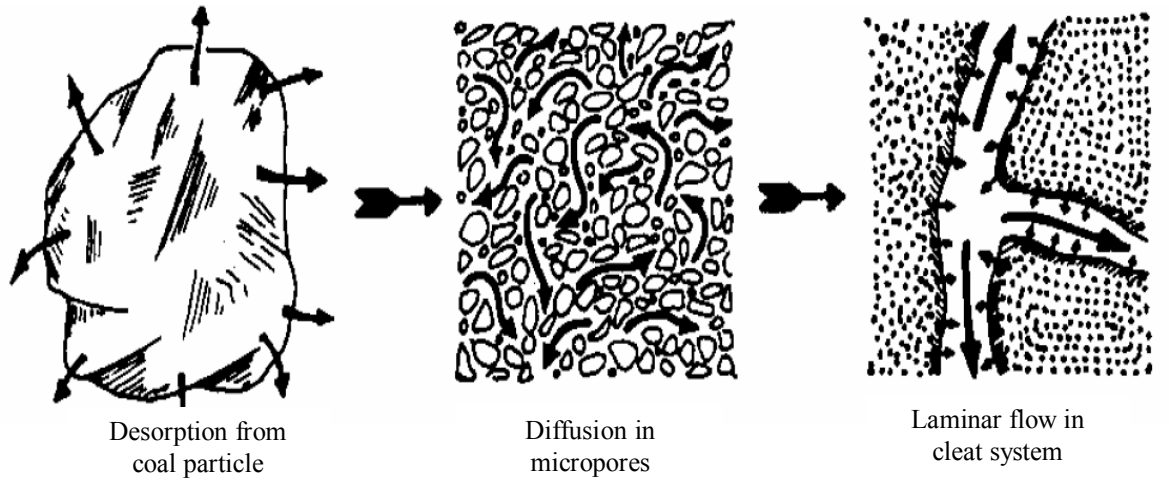

Fig. 3.2 - Methane flow dynamics[11]

Gas transport phenomena at diffusion state can be calculated using Fick's law[34]. At this stage, the gas is transported from the coal matrix micropore system into the fracture system. The coal matrix micropore system is the primary porosity system. In this system the main driving force of the diffusion process is the gas concentration gradient. In the secondary porosity system or fracture system, the fluid flow is governed

by Darcy's law or the pressure gradient. These two transport phenomena are different from each other and yet they are interdependent on each other.

Jochen, V.A., Lee, W.J., and Semmelback, M.E.[35] presented the fundamental equation of the transport phenomena in the secondary porosity system or the macropore system. In the macropore system or the cleat system, the transport phenomena of water and gas are quantified using the following equation:

$$\frac{1}{r}\frac{\partial}{\partial r}\left[\frac{K_g}{\mu_g B_g} r \frac{\partial p_g}{\partial r}\right] + q = \frac{\partial}{\partial t}\left[\phi \frac{S_g}{B_g}\right]$$

whereas the flow rate (q) is formulated as:

$$q = -F_g \frac{\partial C}{\partial t} \quad \text{.....3.1}$$

In this equation, q represents the pseudo-steady state diffusion rate at two given points. The diffusion rate is determined by F_g, a dimensionless shape factor. Each shape factor value represents a different micropore matrix geometry. The diffusion rate is the rate of released gas flows to the fracture system; this phenomenon is governed by the gas concentration gradient. The gas concentration gradient could be expressed by the following equation:

$$\frac{\partial C}{\partial t} = DF_s\left[\overline{C} - C\left(p_f\right)\right] \quad \text{.....3.2}$$

In this equation, $\overline{C}$ is the gas concentration (average in the coal matrix system) and the $C(p_f)$ is the gas concentration (in the fracture system). The gas concentration at a

particular time step is calculated by using a material balance equation. Combining Eqn. 3.1 and Eqn. 3.2, the diffusion rate terms can be illustrated by the following equation:

$$q=-F_g\,D\,F_s\left[\bar{C}-C\left(p_f\right)\right]$$

where F_s is shape factor for the primary porosity system. In this equation the product F_gDF_s also represents the desorption time or the time constant for the pseudo-steady state condition, written as τ. The desorption time is formulated as:

$$\tau=\frac{1}{F_g\,D\,F_s}$$

By using the desorption time term, the equation for diffusion or desorption state is:

$$q=-\frac{1}{\tau}\left[\bar{C}-C\left(p_f\right)\right]$$

The desorption time is a value representing a characteristic of a drainage process which is the required time to desorb 63.2% of the ultimate drainage for a constant pressure and temperature condition[36]. This parameter, (τ), represents the required time for gas to be released from the surfaces area of the internal coal micropores system and transported to the fracture (macropore system). In coalbed methane reservoir modeling, it is more common to quantify the diffusion rate using the desorption time rather than the diffusivity value. Practically, desorption time data could be determined by a laboratory test called the canister test. In this test, coal core samples are placed in a desorption canister equipment and equilibrated to a given temperature while measuring the desorbed gas as the pressure system is decreased at any consecutive time.

Another expression of the diffusion process is presented by using a shape factor. The drainage rate governed by Fick's law can be quantified using the following equation.

$$q^* = \sigma . D_c . \left(\overline{C} - C_f \right)$$

where q^* is the drainage rate per volume of the reservoir. The relationship between the desorption time (τ), shape factor (σ) and diffusivity coefficient (D_c) can be expressed by the following equation:

$$\tau = \frac{1}{\sigma . D_c} \quad \text{.....3.3}$$

After the desorbed gas is released and transported to the fracture system (macropores), the fluid flow is then governed by Darcy's law. The fluid flow within this fracture system can be described as the following equation:

$$q = - \frac{k A}{\mu} \frac{dp}{dL}$$

As shown in this equation, the main driving force of fluid flow through fracture system is the pressure gradient. This is the main difference between the transport phenomena in the matrix system (micropores) and the fracture system (macropores). Although the gas transported from the matrix system follows the concentration gradient (Fick's law), the amount of gas desorbed depends on the system pressure. The amount of gas released at every pressure value follows the Langmuir isotherm curve.

3.4 Adsorption Isotherm

Methane gas is stored in the coal matrix by an adsorption process. The amount of gas adsorbed on the internal surface area of the coal matrix micropore system can be very large since the coal is able to provide a tremendous internal surface area. An analogy for the adsorption process is dust attached to a surface area of wood or glass. The adsorption is governed by the weak attraction forces between molecules. Therefore adsorption process is reversible. Absorption is a different process; it is less reversible than the adsorption process. An example of an absorption process is when water soaks a sponge. The adsorption process may be explained with the Langmuir isotherm curve. The Langmuir isotherm theory perceives gas molecules attached on the surface area as a single layer (monolayer).

The basic concept of Langmuir isotherm theory is that the rate of gas molecules arriving and adsorbing on a solid surface area is proportional to the rate of gas molecules leaving the solid surface area. The Langmuir isotherm curve is useful to predict the amount of gas released at a given pressure lower than desorption pressure. For a gas storage mechanism, Kohler, E.T. and Ertekin, T.[37] presented the relationship between storage capacity and the adsorption isotherm curve. In an adsorption phenomenon conceptual model, the Langmuir isotherm curve theory is applicable in an unconventional gas reservoir, including a coalbed methane reservoir. An example of a Langmuir isotherm curve is shown in Fig. 3.3.

As the system pressure declines, the storage capacity decreases and a certain amount of gas will be released from the matrix system. The maximum storage capacity

is the Langmuir volume, a saturated monolayer volume. At this value, all surface area has been adsorbed by methane gas or the gas content at an infinity pressure value. The Langmuir pressure is a pressure value at half of the Langmuir volume.

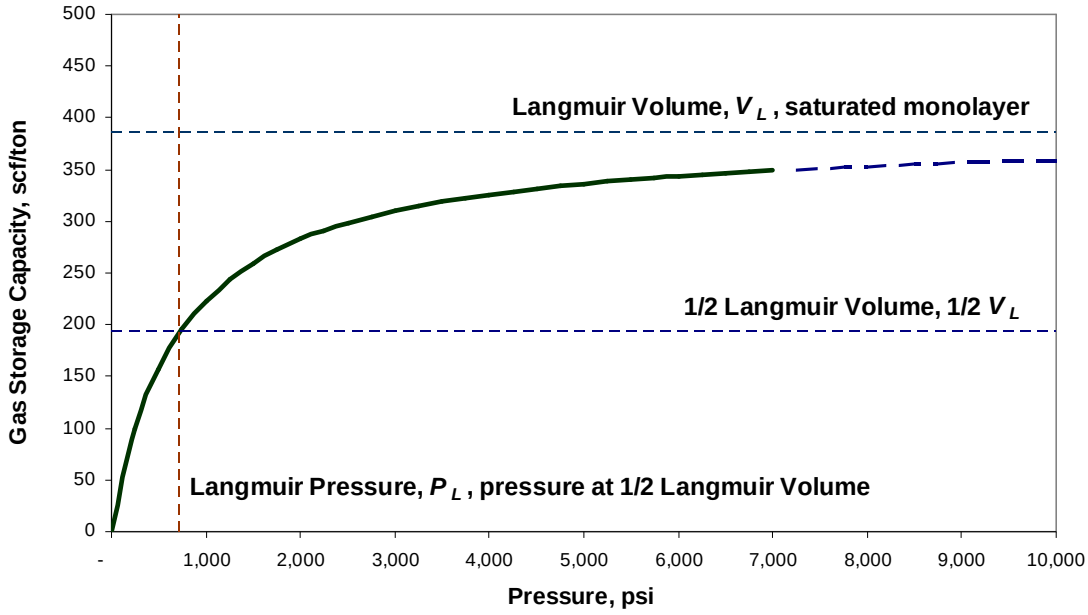

Fig. 3.3 - Sorption isotherm, gas content as a function of pressure

The amount of gas adsorbed on the internal surface area of the coal matrix micropore system could be quantified using the Langmuir equation. The Langmuir isotherm equation is described as the following:

$$V(p)=V_L \frac{p}{p+p_L}$$

where $V(p)$ is the gas content at any given pressure (scf/ft^3), p_L is the Langmuir pressure (psi), p is the pressure in the matrix system (psi) and V_L is the Langmuir volume (scf/ft^3).

The Langmuir volume can be estimated since it asymptotically increases at higher system pressure value. The Langmuir pressure is the pressure value at a condition when the amount of adsorbed gas reaches half of its maximum storage capacity. The Langmuir pressure determines the curvature of the Langmuir isotherm curve. At a lower Langmuir pressure value, the isotherm curve will be lower. However, at any Langmuir pressure values, all curves will coincide at the same value, which is the maximum mono-saturated value.

The Langmuir isotherm equation quantifies the amount of gas released at a given pressure. The gas concentration at a certain pressure is assumed in an equilibrium state. Therefore, in the Langmuir isotherm equation the change of methane gas concentration depends only on pressure reduction. The pressure reduction allows gas to be desorbed and transported through the diffusion process in the micropore system. There is a pressure value when the gas starts to desorb, which is called the critical desorption pressure. If the pressure value is higher than the desorption pressure, the gas desorption process will never be initiated. To reduce the matrix system pressure, formation water should be removed from the fracture system by making a coalbed methane well. Initially, the only produced fluid is formation water. The amount of water being produced is proportional to pressure reduction. After the reservoir pressure system achieves a lower value than the critical desorption pressure, gas starts to be produced at an early low rate and it reaches the peak gas production after several years. This phenomenon is different from a conventional gas reservoir, where the gas production declines without having to wait for the dewatering process.

Fig.3.4. shows a typical coalbed methane production performance. The production profile is typical for an undersaturated coalbed methane reservoir system. An undersaturated coalbed methane reservoir has a higher initial reservoir pressure than the critical desorption pressure. Therefore, a depressurizing stage is necessary to allow the desorption process to initiate. After the desorption process occurs, gas desorbs until it achieves critical gas saturation. At this time gas and formation water flow through the natural fracture system into the wellbore.

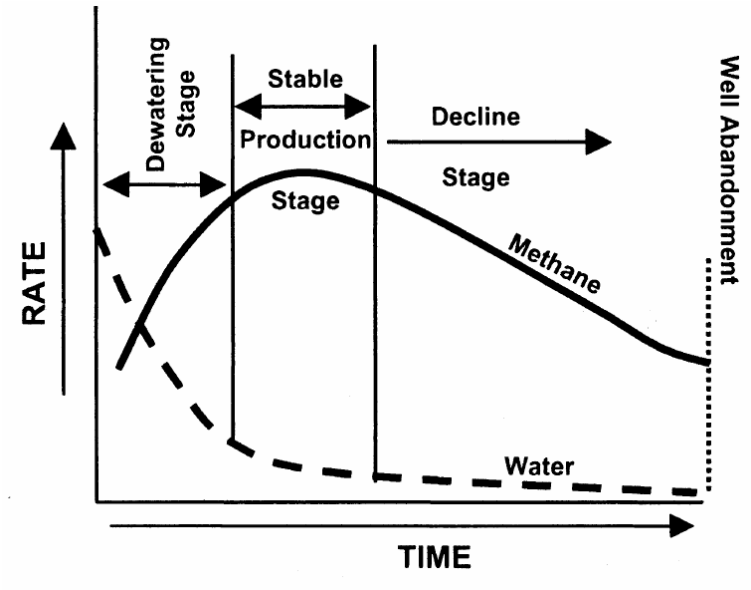

Fig. 3.4 - Typical coalbed methane production performance behavior[4]

3.5 Coalbed Methane Reservoir Porosity

In coalbed methane reservoir, coal formation is considered as both source rock and reservoir rock. During coalification, methane gas is formed and stored in the same media. Unlike in a conventional gas reservoir, where gas migrates from source rock to

reservoir rock, in this unconventional gas reservoir the methane gas is trapped at the same place where it is originated from. In a conventional gas reservoir, the gas is stored in the pore system or void between solid particles. On the other hand, coal is a solid substance with micropore systems inside the coal matrix, surrounded by the natural fracture system or cleat system. In a coalbed methane reservoir, only a small amount of gas is stored as free gas in the pore system. Most of the gas stored as adsorbed gas in the matrix micropore system. The coal micropore system provides a tremendous surface area for methane gas to be stored during the adsorption process.

Basically there are three types of the coal pore system. The first type is the natural fracture system or the cleat system, including the face cleats and butt cleats. This pore system allows gas to be transported from the coal matrix into the wellbore with the pressure gradient as a driving force. Another type is the interstitial pore space in the coal matrix system. In this pore type, gas is stored as free gas inside the pore throat. The coal matrix also has another type of porosity, the micropore system. The micropores are very small in size yet able to provide a large amount of surface area to attach gas molecules.

3.6 Coalbed Methane Reservoir Permeability

A coalbed methane reservoir is commonly identified as a naturally-fractured reservoir. Coal seams consist of the matrix system and fracture system. The matrix system is the main methane gas storage but with very low permeability. Since the permeability value is very low, it is often neglected in the modeling concept. Even when gas transport phenomena occur in the matrix system, the gas drainage rate is very slow

and is dominated by the diffusion process (Fick's law) instead of the fluid flow through permeable media (Darcy's law). Therefore, in a coalbed methane reservoir the permeability concept is only applied in the fracture system. The coal permeability in the fracture system determines how fast the depressurizing process will take place by removing formation water from the fracture system.

3.7 Coalbed Methane Reservoir Saturation

In coalbed methane reservoir modeling, a gas and water saturation concept is only applied in the coal micropore system. A coalbed methane reservoir consists of a macropore system (fracture or cleats) and a micropore system (coal matrix). Initially, the fracture system is fully saturated with water. It is common to neglect gas presence in this early stage. After the desorption process begins, gas saturation in the fracture system increases until it reaches the critical gas saturation. After achieving gas saturation value higher than the critical gas saturation, methane gas starts to flow from the fracture system into the wellbore and is exploited through surface facilities. Therefore, in a coalbed methane reservoir, saturation terms refer only to the fracture or cleat system.

3.8 Coalbed Methane Reservoir Permeability Anisotropy

There are numerous authors who have introduced the existence of permeability anisotropy in a coalbed methane reservoir. The main path for the fluid flow inside the coal seam is the cleat system. Since there are two kinds of cleat systems in a coalbed methane reservoir, the direction of permeability is complicated. The face cleat is more continuous and it contributes a larger surface area for a gas drainage process from the

matrix system to the fracture system. The face cleat direction is perpendicular to the butt cleat direction. The butt cleat system is the shorter natural fracture system intersected by face cleat systems. Therefore the existence of face cleats system and butt cleats system yield permeability anisotropy in the coalbed methane reservoir system. The well pattern should consider permeability anisotropy in order to obtain the most optimum drainage within a reservoir body.

Some authors have presented the significance of permeability anisotropy in drainage pattern. Wicks, D.E., Schewerer, F.C., Militzer, M.R., and Zuber, M.D.[32] presented a drainage pattern and methane gas recovery in a coalbed methane reservoir. Based on their result, the rectangular drainage pattern increases methane gas recovery up to 15 percent compared to the square pattern. Bumb, A.C. and McKee, C.R.[38] also presented the beneficial effect of designing a well pattern with the permeability anisotropy in consideration. They showed that an appropriate well pattern would increase the effectiveness of dewatering process.

Sung, W., Ertekin, T., and Schewerer, F.C.[39] used a numerical reservoir simulator to study the effect of well trajectory direction to methane recovery. They proposed to drill a vertical well in the face cleat direction to improve methane recovery. Another study by Young, G.B.C., McElhiney, J.E., Paul, G.W., and McBane, R.A.[30] showed the importance of a permeability anisotropy study in developing a coalbed methane reservoir in Cedar Hill Field, Northern San Juan Basin. Following their study result, methane gas recovery can be improved by designing well placement with the

permeability anisotropy in consideration. They used a numerical simulator to model permeability anisotropy and coalbed methane reservoir production performance.

Chaianansutcharit, T., Her-Yuan Chen, and Teufel, L.W.[33] also studied the permeability anisotropy effect on methane recovery in a coalbed methane reservoir. They also introduced the dual peak gas rate behavior caused by boundary effects. The dual peak gas rate occurs in a coalbed methane reservoir system with several boundaries with different required times to achieve the boundary effect. They also suggested using a rectangular drainage pattern in a coalbed methane reservoir development strategy.

3.9 Numerical Reservoir Model

Naturally fractured reservoir model consists of two different sub-systems: the matrix system, which contributes to pore volume, and the fracture system, which is the main path for the fluid flow. These two sub-systems are dependent on and interconnected with each other. This concept is known as a dual porosity model. The matrix system and fracture system have distinct characteristics, as presented by Warren and Root in 1963[8]. They introduced an idealized model for the dual porosity system. However, there is a distinguished concept in a coalbed methane reservoir. Unlike in a conventional gas reservoir, the matrix system has very low permeability.

The gas transport phenomenon in a coalbed methane matrix system is different from the fluid flow mechanism in the fracture system. The gas drainage rate is very low and dominated by the diffusion process. Therefore, to accommodate these unique characteristics the Warren and Root model should be modified in coalbed methane reservoir modeling. The modified dual porosity model should take into account the

diffusion process from the matrix system to the fracture system. This physical process can be quantified by Fick's law. Unlike the dual porosity model in a conventional reservoir, the dominant driving force in matrix system is the gas concentration gradient.

In a conventional gas reservoir, the fluid flow mechanism in the matrix system depends on the matrix pressure and the gas saturation in the matrix system. However, the gas releasing mechanism in a coalbed methane reservoir depends on pressure. As the matrix pressure declines, more gas will be released from the internal surface of the matrix micropore system.

Even though the dual porosity concept is applicable in a coalbed methane reservoir, the fundamental is different. Referring to the dual porosity concept, the matrix system also contributes to the fluid flow although the porosity and permeability value is very low. In a coalbed methane reservoir, the porosity and permeability concept is not appropriate to be used in the matrix system. The effective permeability and porosity in the coal matrix system is negligible. However, the matrix system is the main source of methane gas. The drainage process refers to methane transport phenomena in the matrix system depending on gas concentration gradient. The gas concentration depends on system pressure. Considering that the matrix system only contributes in gas source terms, a coalbed methane reservoir can be modeled by the single porosity system coupled with the pressure-dependent gas source term.

An idealized model of a coalbed methane reservoir system is shown in Fig. 3.5. A picture of an actual coal seam is presented in the left side. A face cleat is a continuous fracture system longer than a butt cleat. The butt cleats are shorter and intersected by

face cleats. To build a reservoir model the cleats system is presented by a systematic array of matrix blocks surrounded by fractures.

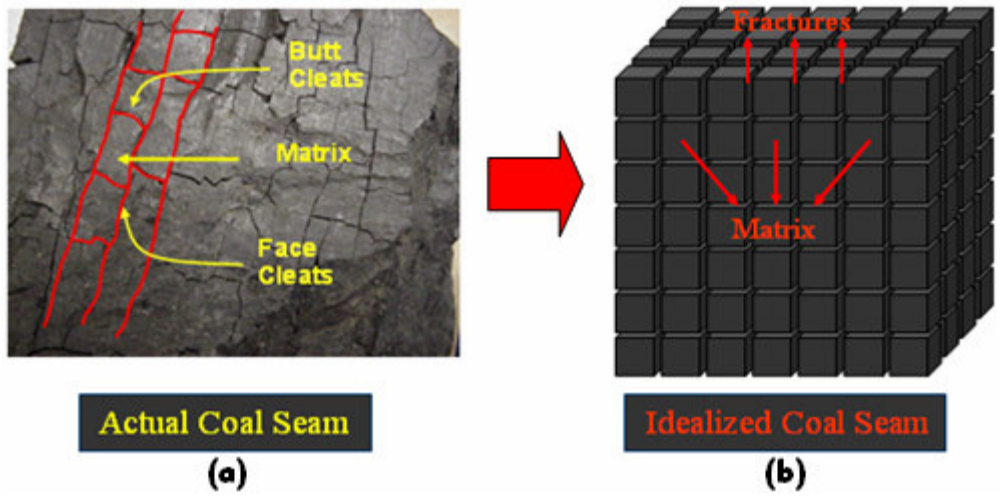

Fig. 3.5- Idealized coal seam model based on the dual porosity concept. (a) an actual coal seam and (b) an idealized coal system model [4]

The matrix block permeability is very low but it has a high gas storage capacity at the adsorption state. The matrix storage capacity is very large due to its ability to provide a tremendous amount of internal surface area for methane gas to be adsorbed. The adsorption process depends on the matrix system pressure. The fracture system permeability is much higher, provides the main path for the fluid flow, and has negligible gas saturation.

This work uses CMG GEM, a two-phase compositional simulator to model coalbed methane reservoir performance under various well-spacing scenarios. This simulator is suitable for the gas diffusion model in the matrix system. A dual-porosity model is used to calculate the mass transport phenomena between the matrix system and the fracture system. In the matrix system, the desorption process is quantified by using

the Langmuir sorption isotherm theory. The fluid flow in the fracture system is modeled by Darcy's law. Instead of Darcy's law, the matrix-to-fracture flow model uses the diffusion theory. By understanding this concept, the permeability value in the matrix system is redundant. On the other side, the matrix relative permeability data are also redundant in the matrix system.

In CMG GEM, the dual-porosity model uses Gilman and Kazemi finite difference equation[40]. The diffusion process is quantified by the gas concentration gradient based on the Langmuir isotherm model. The gas drainage through the diffusion process is calculated using the Fick's law. On the other hand, the gas concentration depends on the system pressure. Therefore, an equilibrium condition between gas concentration at any given pressure and the drainage rate is calculated during the iteration process or each time step. This simulator has also incorporated coal shrinkage and compaction effect during the reservoir life.

The mass transport phenomenon from the matrix system to the fracture system or diffusion process is unique for each coal type. A parameter called the desorption time (τ) determines how fast the drainage process during diffusion process. The desorption time could be calculated based on the diffusion coefficient, cleat spacing, and shape factor. CMG uses Kazemi's concept to calculate the shape factor. For a very low value of desorption time, the diffusion process will be faster and the equilibrium state can be achieved within a shorter time.

Even permeability and relative permeability data are not required for the matrix system; the simulator needs input data for the dual-porosity model. The dual porosity

model consists of two different porosity systems. The primary porosity is the matrix system and the secondary porosity is the fracture system. In coalbed methane reservoir modeling, it is necessary to understand that the concepts of permeability and relative permeability are only applied in the fracture system. The matrix system only provides the gas source and the amount of released gas during the desorption process depends on matrix pressure at a given time.

CMG GEM as a compositional simulator is able to provide a numerical simulation model for a coalbed methane reservoir. However, one should be careful in utilizing the dual-porosity concept in this simulator since it is different from its use in a conventional gas reservoir. The mass transport phenomenon in the matrix system is different from the conventional simulator where the permeability and relative permeability values determine the fluid flow in the matrix system.

3.10 Sensitivity Study

To investigate and mitigate the risks in coalbed methane reservoir development, one should have adequate understanding about relationship between the uncertainty of reservoir properties and their impact on production performance. A sensitivity study is widely used in the procedures of finding the relative importance of each parameters and their inter-relationship. The main purpose of conducting this study is to build a rank correlation between the parameters and the expected outcome (e.g. cumulative gas production, recovery factor, original gas in place). There are several methods commonly

taken to perform sensitivity study, such as the One-Factor-A-Time method, the Placket Burman method, and the Box Behnken method.

3.10.1 One-Factor-A-Time Approach

A sensitivity study is performed by changing one factor at a time while keeping the other factors constant during calculation. This method has been quite popular because of its simplicity and tendency to avoid mistakes during calculation. However, this method is limited in term of its capability to investigate all extremities of input parameters.

The extreme condition for some cases occurs when a combination of input parameters is introduced. For example, gas production will increase with higher fracture system permeability. The maximum effect of changing fracture permeability cannot be observed only by changing the fracture permeability alone without changing other input data. For this case, higher gas production can be obtained by maximizing the fracture permeability and reservoir thickness. Table 3.1 shows an example of the One-Factor-A-Time approach.

3.10.2 Plackett-Burman Approach

The Placket-Burman approach is categorized as a two-level factorial design. In a two-level factorial design, there are two values of each parameter that will be taken into account in a sensitivity analysis. Those values are the minimum value and maximum value. For a complete combination, the n factor requires 2^n experimental runs to consider

all possible combinations among all the factors. For example, to make sensitivity analysis for 3 factors, one should prepare 8 experimental runs. The advantage of using the Plackett-Burman design is to reduce the amount of experimental runs. The Plackett-Burman design introduces a single generating vector to construct a certain number of experimental runs. Table 3.2 shows generators used in Plackett-Burman design. The minimum condition is symbolized by -1, while 1 means maximum condition[41].

Table 3.1 - Example of one factor at a time appoach

Parameter	Minimum	Most Likely	Maximum
Thickness, ft	*25*	30	*40*
Matrix porosity, fraction	*0.0125*	0.005	*0.2*
Fracture porosity, fraction	*0.0025*	0.001	*0.04*

Experiment	Thickness, ft	Matrix porosity	Fracture porosity
1	30	0.005	0.001
2	*25*	0.005	0.001
3	*40*	0.005	0.001
4	30	*0.0125*	0.001
5	30	*0.2*	0.001
6	30	0.005	*0.0025*
7	30	0.005	*0.04*

Table 3.2 - Plackett-Burman design generator

Number of Factors	Number of Runs	Generator
4 - 7	8	1 1 1 -1 1 -1 -1
8 - 11	12	1 1 -1 1 1 1 -1 -1 -1 1 -1
12 - 15	16	1 1 1 1 -1 1 -1 1 1 -1 -1 1 -1 -1 -1
16 - 19	20	1 1 -1 -1 1 1 1 1 -1 1 -1 1 -1 -1 -1 -1 1 1 -1
20 -23	24	1 1 1 1 1 -1 1 -1 1 1 -1 -1 1 1 -1 -1 1 -1 1 -1 -1 -1 -1 -1
32 - 35	36	-1 1 -1 1 1 1 -1 -1 -1 1 1 1 1 1 -1 1 1 1 -1 -1 1 -1 -1 -1 -1 1 -1 1 -1 1 1 -1 -1 1 -1

3.10.3 Box Behnken Approach

When there are three conditions available in one parameter, a three-level factorial design is required. Examples of the three conditions are the minimum value, the most-likely value, and the maximum value. The Box Behnken method is one approach that is categorized as a three-level factorial design. A three-level factorial design uses all combinations among three factors. For a complete design, one needs to prepare 3^n

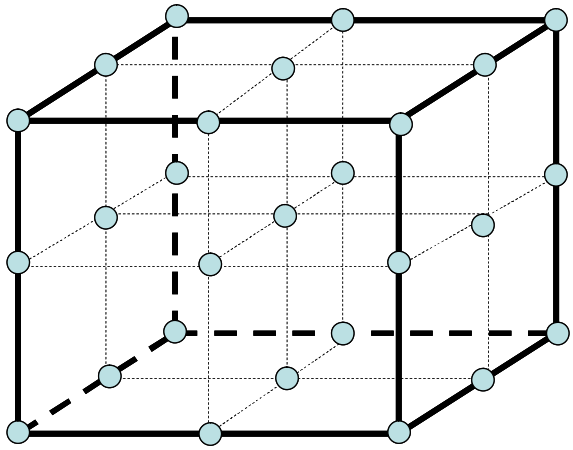

Fig. 3.6 - Illustration of Three-level full factorial design

experimental runs for n factor. For instance, 3 factors will need 27 experimental runs to have a full factorial design. A graphical illustration of full factorial design is presented in Fig. 3.6.

One of the advantages of using the Box Behnken method is that the required experimental runs will be much less than a three-level full factorial design. The Box Behnken method is also very useful in selecting fewer experimental runs to provide responses of the main effect from each parameter. This method also considers

relationship between a parameter and all quadratic effects. The disadvantage of Box Behnken method is its inability to investigate the extreme condition. Fig. 3.7 shows an illustration of the Box Behnken approach.

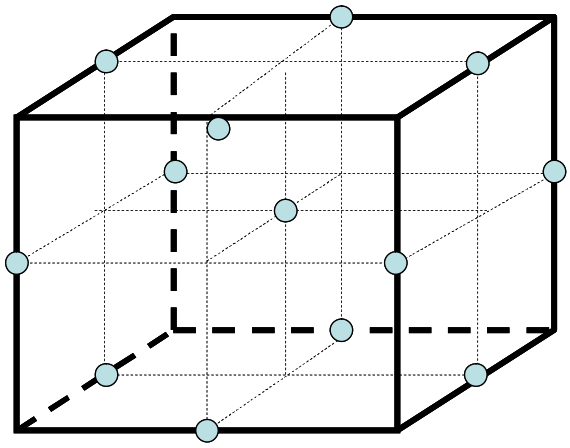

Fig. 3.7 - Illustration of Box Behnken design

3.11 Monte Carlo Simulation

The Monte Carlo simulation has been widely used to accommodate uncertainties in reservoir engineering. Each parameter has uncertainty. It is common to provide reservoir data in a range of more than a single value. The Monte Carlo simulation can be used to transform the uncertainty from a selected parameter to produce a distribution function. Each parameter has a distribution function and when all the distribution functions are combined, the result will be different. To sample a number of input data, random numbers are generated. A graphical presentation is shown in Fig 3.8 to illustrate distribution functions as a result from the Monte Carlo simulation.

There is a concession in the cumulative distribution function to have a description about the expected value. The P10 (also being known as proven) value

represents a certain value where there is 10% possibility to acquire values less than the P 10 value. The same concept applies for P 50 (probable) and P 90 (possible).

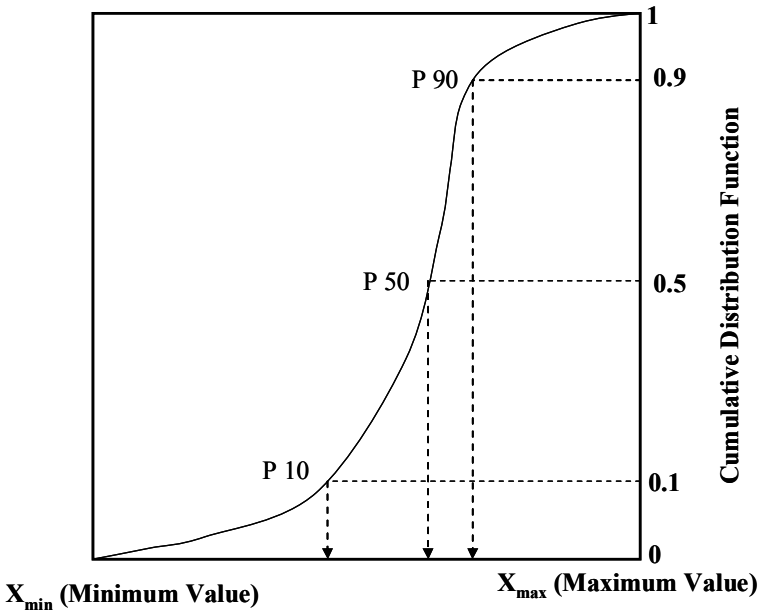

Fig. 3.8 - Typical Monte Carlo simulation result

The uncertainty of each parameter is defined as a distribution function. For three values (including the minimum, maximum, and most likely value), a triangle distribution is usually applied in the input data. Examples of a triangle distribution are presented in the following figures. Fig. 3.9 illustrates any data smaller than the most likely value and Fig 3.10 represents any data bigger than most likely value.

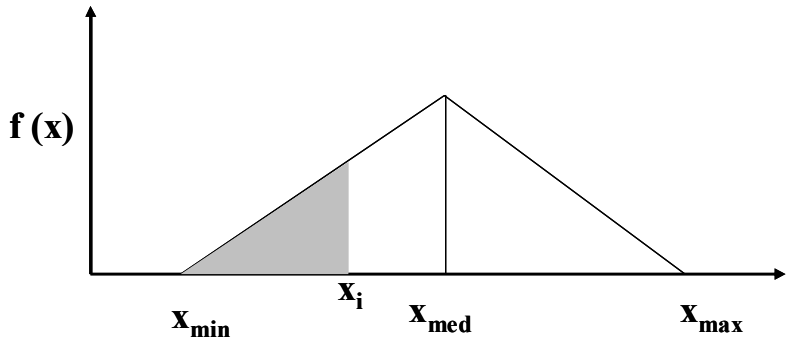

Fig. 3.9 - Triangle distribution for a value less than medium, ($x_i \leq x_m$)

The formula to calculate the value between the minimum value and the most likely value is:

$$x_i = x_{\min} + \sqrt{(x_{\max} - x_{\min})(x_m - x_{\min})\,R_n}$$

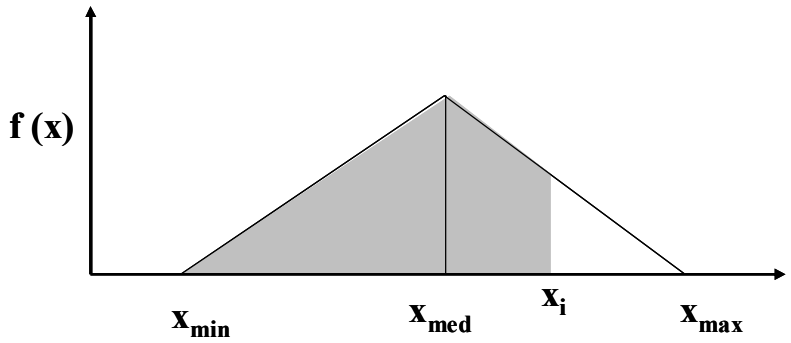

Fig. 3.10 - Triangle distribution for a value more than medium, ($x_i \leq x_m$)

The formula to calculate the value between the minimum value and the most likely value is:

$$x_i = x_{\max} - \sqrt{(x_{\max} - x_{\min})(x_m - x_{ml})\,R_n}$$

CHAPTER IV

WELL SPACING STUDY RESULTS AND ANALYSIS

4.1 Introduction

A coalbed methane reservoir has very distinct characteristics in terms of the dewatering process. A dewatering stage needs to be done to reduce reservoir pressure. As the reservoir pressure decreases at a certain stage, gas desorbs from the coal matrix. However, in a dry coal reservoir system, the dewatering phase is not necessary. The uncertainty of a dewatering phase plays an important role in the feasibility of a coalbed methane reservoir development plan.

In the early stage of coalbed methane reservoir development, it is very important to have an initial estimation about the initial cost and the total revenue. An economic model gives an illustration about a project feasibility. In a very limited data situation, a sensitivity study provides understanding about the influence of reservoir properties to the economic model. A sensitivity study also gives illustration about the influence of each reservoir property to the prediction of gas production. Another importance of performing a sensitivity study is to find the most influential factors that govern the overall project economic calculation.

To evaluate a coalbed methane reservoir development project, one of the most important sequences is to forecast the methane production performance. Different from a conventional reservoir, a coalbed methane reservoir has a dewatering stage and it is difficult to estimate gas production based only on the decline curve analysis. The best

way to estimate gas production is to conduct a numerical reservoir simulation. To a great extent, some reservoir properties such as the gas content and coal permeability will affect coalbed methane reservoir production performance. However, there are also other reservoir properties with minor influence, for example the reservoir temperature. Determining the range of each parameter will also govern the influence of each parameter itself. For instance, the coalbed reservoir thickness has a direct influence to total gas production; but in a special case, when the range is narrow, the effect of varying thickness is also insignificant.

In the early development of a coalbed methane reservoir, determining well spacing is very important. The well-spacing scenario dictates the amount of producing wells that will be required to develop the reservoir in the optimum condition. The initial investment also depends on the well-spacing strategy. In fact, the well-spacing strategy regulates the overall drilling cost which is the largest portion of the initial investment. This chapter proposes a procedure to evaluate well spacing scenario in the early stage of coalbed methane reservoir development.

4.2 Sensitivity Study

As an example of a sensitivity study, a data set from San Juan Basin is selected. This data set does not represent the general characteristics of the San Juan Basin coalbed methane reservoir but only its particular area. The reservoir depth is about 3280 ft with saturated water in the fracture system and the initial reservoir pressure of 725 psi. A

dewatering stage is necessary in the early production stage. The following data set will be a base case for further sensitivity study (Table 4.1).

A radial angular cylindrical grid is prepared to construct a single well, vertical completion model. A reservoir is modeled by 31 x 1 grid size. In a single-well solution and radial grid system, the finite-difference accuracy can be increased by using geometrically spaced radial grids. This grid system provides a better solution for the constant pressure or the constant rate boundary especially within the radius of up to a half distance to the boundary. For the outer grid outside the first half distance to the boundary, an equally-spaced grid can be used. The main purpose of using a geometrically-spaced grid system is to get a better pressure profile near wellbore since this area may have a faster pressure change. The well drainage radius is 1,053 ft or 80 acres well spacing.

A compositional simulator module from CMG (GEM) is used to perform a numerical reservoir simulation for the base case data set. The simulation runs with a constant pressure boundary of 14.7 psi at the bottom hole. The numerical simulation model is shown in Fig. 4.1 while Fig. 4.2 shows the simulation result for the particular base case.

A typical coalbed methane reservoir production performance occurs in the simulation result. In the early stage, the dewatering process is obtained by producing water at an initial rate of 93 bpd and it rapidly declines to less than 10 bpd in 5 years production. The gas production rate culminates in the amount of 205,500 scfd after 640

days, which is followed by decline and behavior as found in a conventional reservoir. After 20 years of production, the gas rate will be at 31,634 scfd.

To perform a sensitivity study, certain ranges of data sets are selected. The ranges do not represent the general characteristics of the San Juan basin coalbed methane reservoir. However, the data are taken form SPE papers with San Juan Basin as the

Table 4.1 - Dataset for base case

Parameter	**Value**	**Unit**
Thickness	30	*ft*
Fracture cleat spacing	0.042	*ft*
Fracture porosity	0.003	
Fracture permeability	1	*md*
Fracture compressibility	$100E^{-6}$	psi^{-1}
Matrix porosity	0.005	
Matrix permeability	0.1	*md*
Matrix compressibility	$100E^{-6}$	psi^{-1}
Water density.	62.4	lb/ft^3
Water viscosity	0.607	*cp*
Water compressibility	4E-06	*cp*
Coal density	89.5841	lb/ft^3
Langmuir volume	0.23	*gmole/lbm*
Langmuir pressure	725.189	*psi*
Desorption time	10	*Days*
Initial pressure, Fracture	1109.54	*psi*
Initial water saturation, Matrix	0.592	
Initial water saturation, Fracture	0.999	
Reservoir temperature	113	*°F*
Depth	3280	*ft*

reference. The ranges are not equally distributed for all parameters, for example, the fracture permeability value ranges from 0.1 md to 50 md. The increment of the permeability value in this case is about 500 times (from the lowest case to the highest case). On the other hand, the thickness varies from 6.8 ft to 40 ft, which is less than the a hundred times difference between the lowest case to the highest case.

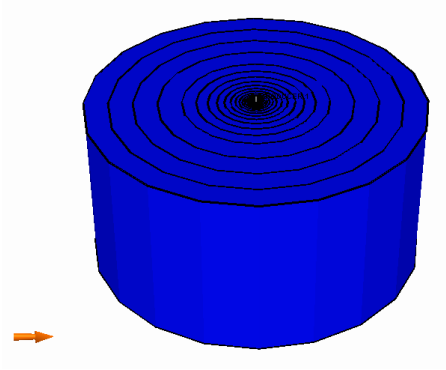

Fig. 4.1 - Geometrically spaced radial grid system for 31 grid blocks

The Langmuir volume gives estimation of gas content in the coal matrix. The values for the Langmuir volume are between 100 scf/ton and 669 scf/ton. Fracture cleat spacing defines the width or aperture between natural fractures in the coal matrix. This parameter has a direct influence to fluid flow in the fracture system. The fracture cleat spacing in the sensitivity study is between 0.017 and 0.05 ft. The initial water saturation in the fracture system is various between 0.77 and 1 (100% fully saturated with water). To model the formation damage, the input data for skin factor are between -6 and 0 (no damage) and 6 (damage).

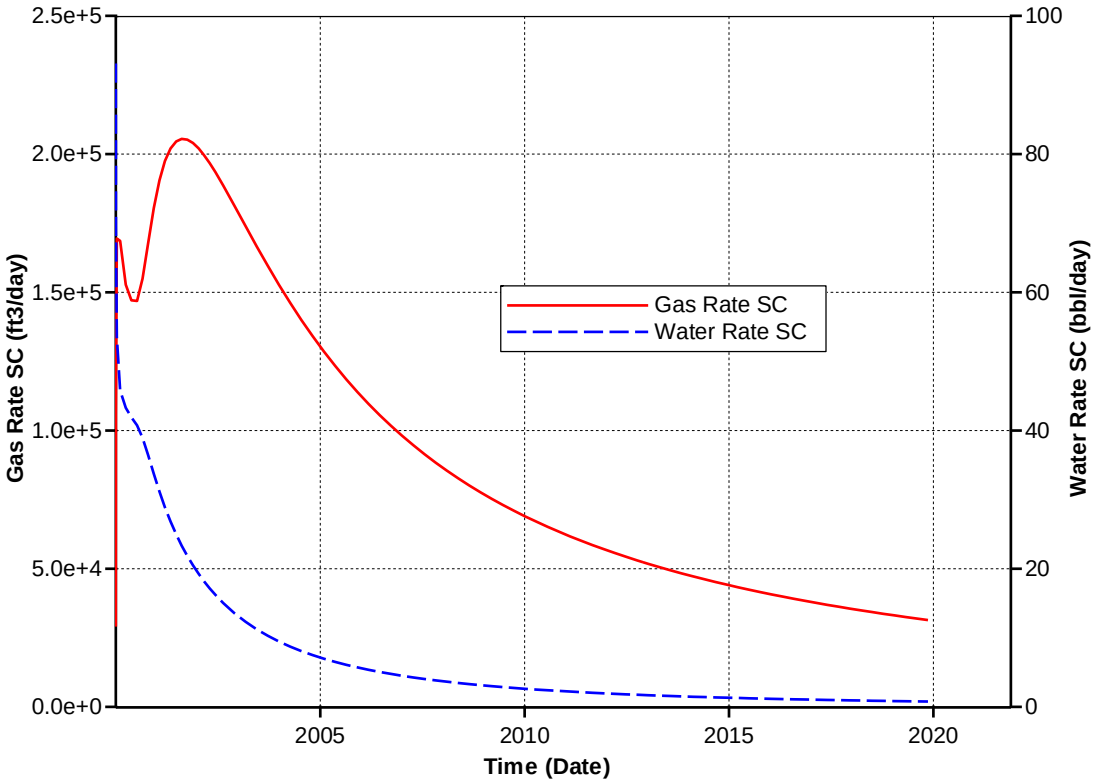

Fig. 4.2 - Reservoir simulation result of base case data set

After determining a particular range for each parameter, a sensitivity study is then commenced. Table 4.2 shows the parameter range that has been used in the sensitivity study. The main purpose of conducting a sensitivity study is to have a better insight about the degree of the influence of each parameter. Hence, one can establish a rank among all parameters and focus on improving measurement to obtain a more valid value. For example, if the coal permeability really affects the production performance in a great degree, an additional measurement technique should be performed in the initial

stage of coalbed methane reservoir development (e.g. by conducting whole core analysis or pressure transient testing).

This work uses two methods to perform screening by sensitivity. The screening should be conducted to all parameters to measure the influence of each parameter to the production performance based on particular range. The first method is the One-Factor-at-a-Time and the second is the Plackett-Burman method. For the base case and all other cases, the well spacing is 80 acres. As a response of simulation result, this study uses cumulative production after 20 years divided by the well spacing area, to obtain the cumulative production per acre.

Table 4.2- Parameter range

Parameter	Min	Base	Max
Thickness, *ft*	6.8	30	40
Matrix porosity, *fraction*	0.0025	0.005	0.04
Fracture porosity, *fraction*	0.0025	0.003	0.3
Matrix permeability, *md*	0.01	0.1	1000
Fracture permeability, *md*	0.1	1	50
Fracture cleat spacing, *ft*	0.017	0.042	0.05
Matrix compressibility, 10^{-6} *psi-1*	10	100	200
Fracture compressibility, 10^{-6} *psi-1*	10	100	200
Water density. lb/ft^3	62.4	62.4	62.7
Water compressibility, psi^{-1}	2E-06	3E-06	4E-06
Water viscosity, *cp*	0.550	0.607	0.730
Reservoir temperature, *°F*	68	113	114
Coal density, lb/ft^3	81.00	89.58	109
Langmuir volume, *gmole/lbm*	0.06	0.23	0.4
Reciprocal Langmuir pressure, psi^{-1}	0.001	0.0014	0.0032
Desorption time, *Days*	5	10	20
Initial pressure, *psi*	339	1110	1422
Initial water saturation, *Fracture*	0.77	0.999	1
Initial water saturation, *Matrix*	0.1	0.592	1
Skin	-6	0	6

As a methodology, the One-Factor-A-Time method is very common and it has been widely used as a sensitivity study tool. For every number of parameters, each one has 3 values: the minimum value, the most likely value, and the maximum value. A base case is a result of all parameters in the most likely value. To obtain the influence of each parameter, one can change the value from the most likely value to extreme value only for one parameter at a time while keeping the other parameters in the same value (the most likely value). The advantage of this method is its simplicity and tendency to avoid mistakes during experiment or simulation. However, the relationship between different parameters cannot be recognized. The basic assumption in performing the One-Factor-A-Time method is independent probability condition. It means each parameter does not influence the result of any other parameter whether it is in the minimum value or the maximum one.

Fig. 4.3 shows the One-Factor-A-Time result for 20 factors. To determine the effect of each parameter, 41 simulation runs including the base case have been conducted. A detailed simulation result is available in Appendix B.

Based on the study result, the fracture permeability is found to be the most influential factor. However, the fracture permeability range itself should be considered. In the simulation result of this study, the difference between the minimum value to the maximum value is 500 times. The fracture permeability has a strong relationship with the production performance. The fluid flow from the cleat system can be described using the Darcy's flow evaluation. The fracture permeability is one factor in Darcy's flow

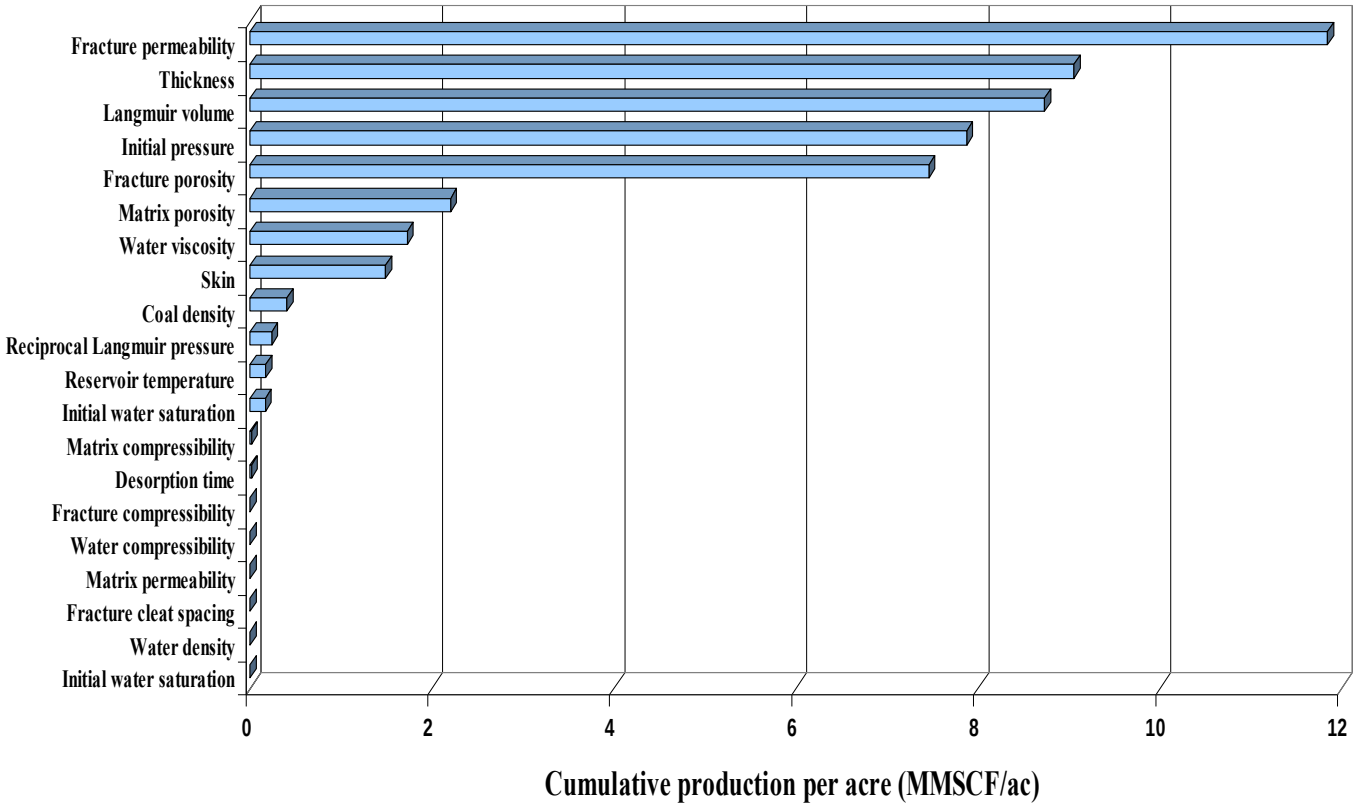

Fig. 4.3 - One-Factor-A-Time sensitivity study result

equation that affects the production performance. Based on this sensitivity study result, coal seam thickness is found to be the second most influential factor. Coal seam thickness value ranges from 6.8 ft to 40 ft. For 67 times of coal seam thickness increment, the cumulative gas production per acre increases from 1.855 MMSCF to 10.909 MMSCF. It means that cumulative gas production strongly depends on the coal seam thickness.

Another factor that creates a big impact on gas production is the Langmuir volume. The Langmuir volume provides an estimation of gas content in the coal matrix. A higher Langmuir volume value will increase the gas production performance.

Another sensitivity study method is Plackett-Burman. This method is also categorized as a "two-level factorial design". The main difference between the One-Factor-A-Time approach and the Plackett-Burman approach is that in the latter the combinations of all factors are taken into consideration.

Since a "two-level factorial design" investigates all combinations of each parameter, the relationships between factors are taken into account. A detailed calculation result of this method is available in Appendix C. In addition to being known as sensitivity study, Plackett-Burman is also recognized as a screening tool. A sensitivity study result based on Plackett-Burman method is shown in Fig. 4.4.

4.3 Economic Model

In carrying out a well-spacing study, it is compulsory to establish an economic model. The economic model needs an estimation of the initial cost, including the operational expenses and capital expenses. The operational expenses comprise the production well maintenance, work over activities (in the average cost per well per month), compression and pumping costs, safety, monitoring and verification activities. Table 4.3 shows assumptions of single-well economic parameters for the economic calculation. The capital expenditures cover production wells (US$ per feet for drilling and completion cost), work over (US$ per feet), pipeline installations (US$ per in-miles), pumping and compression costs. The monthly revenue is calculated based on estimated gas production per month and gas price. With an assumption of 1050 MMBTU/SCF, the gas price is 4 US$/MMSCF. The discount rate is assumed as 10% and the production tax 4.6%.

Since reservoir properties vary based on each range, the outcomes of the estimated production performance also vary. The production performances will be different for each data set. A regression model is constructed from the sensitivity study result. In this work, not all of parameters will be considered to have a significant effect on the production performance. The main idea of this procedure is to obtain a good regression result, and fewer variables tend to have a better regression result. In the One-Factor-A-Time method, 3 factors are taken into account in the regression model (Table 4.4).

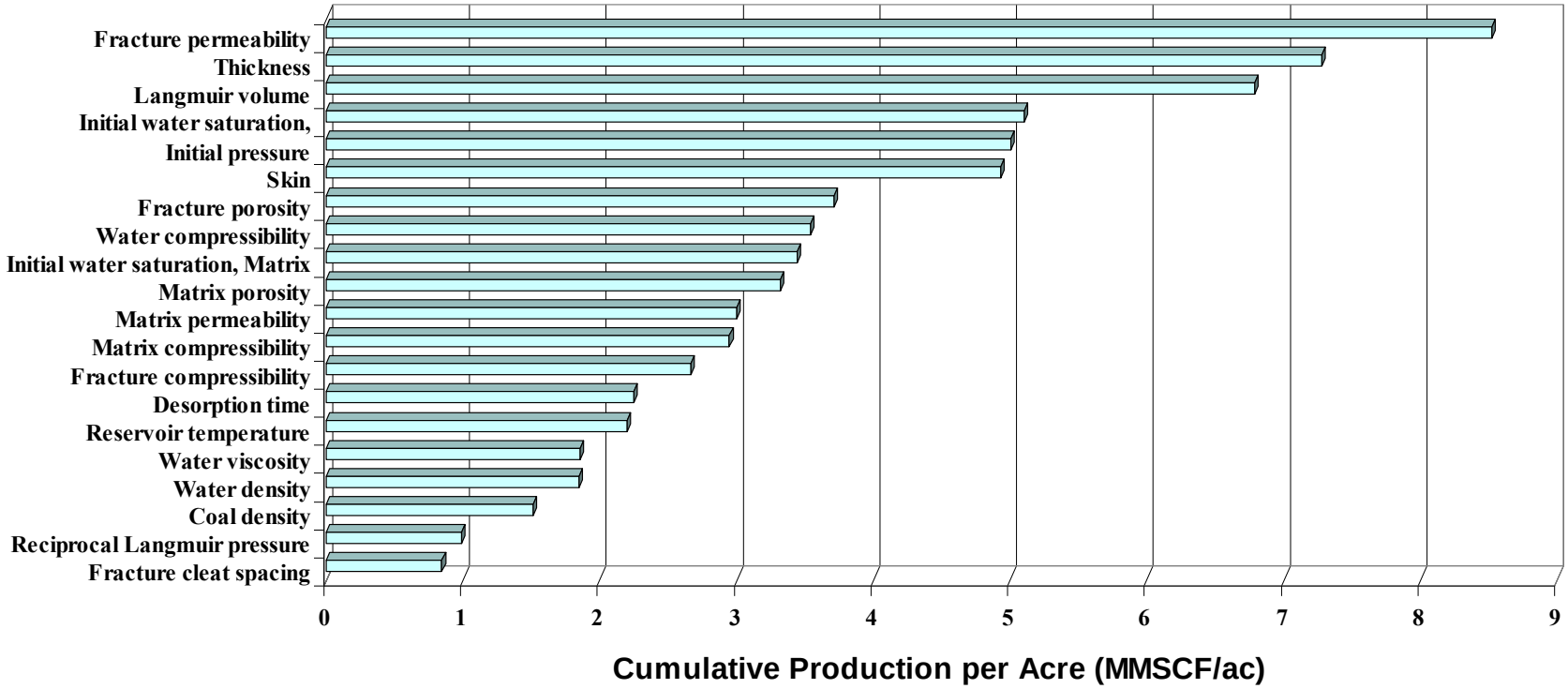

Fig. 4.4 – Plackett-Burman sensitivity study result

Table 4.3 - Single well economic parameters		
Parameter	**Value**	**Unit**
General Data		
Depth :	3280	ft
Gas Heating Value :	1050	MMBTU/SCF
Gas Price :	4	US $/MMBTU
	0.004	US $/SCF
Pipeline Length :	1	in-mile
Compression Power :	20	BHP
Pump Power :	20	BHP
Economic Parameters		
Discount Rate :	10	%
Production Taxes :	4.6	%
Capital Expenditures		
Production Wells :	100	US $/ft
Workover :	100	US $/ft
Pipeline :	20	US $/in-mile
Compression :	1500	US $/BHP
Pumping :	200	US $/BHP
Total Capex :	689,980	US $
Operational Expenditures		
Production Wells :	100	US $/mo
Workover :	10	US $/mo
Compression :	0.1	US $/Mcf
Pumping :	0.3	US $/ton
Safety, Monitoring, Verification :	100	US $/well/year
Total Opex :	1420	US $/year

Table 4.4 - Data set for one factor at a time regression model				
Parameter	**Notation**	**Minimum**	**Most Likely**	**Maximum**
Fracture permeability, md	*F5*	0.1	1	50
Thickness, ft	*F1*	6.8	30	40
Langmuir volume, *gmole/lbm*	*F3*	0.06	0.23	0.4

By using the One-Factor-A-Time method, there are 7 simulation runs available to build a regression model. One case for the base and the other 6 cases represent the extreme values (maximum and minimum). To perform a regression model, this work uses the EREGRESS[Eregress] software application. The Net Present Value (NPV) is calculated from the cash flow in 20 years gas production. The selected regression equation is as follows:

$$NPV = -3303000 - 190161F1 + 44942.7F2 + 3790000F3 + 1897000\sqrt{F1}$$

Based on the regression result, a graphical evaluation is presented in Fig. 4.5. The regression result quality is shown by matching the result with the 45-degree line. Fig. 4.5 shows the quality of the regression model compared to the simulation result. Based on the regression software calculation, R^2 is 0.997. In a statistical model the R^2 value represents how well the equation can predict the future outcome of a model, in this case, the reservoir simulation model. The regression model represents the reservoir simulation result for all values within the range. This regression model is utilized to perform a Monte Carlo simulation.

To conduct a Monte Carlo simulation, 10,000 random numbers are prepared. After obtaining the Monte Carlo simulation result, a cumulative distribution function is constructed. The main reason of providing the cumulative distribution function is to have estimation about the economic value of each well-spacing scenario. Fig. 4.6 shows the cumulative distribution function of the One-Factor-A-Time method for 80 acres well spacing.

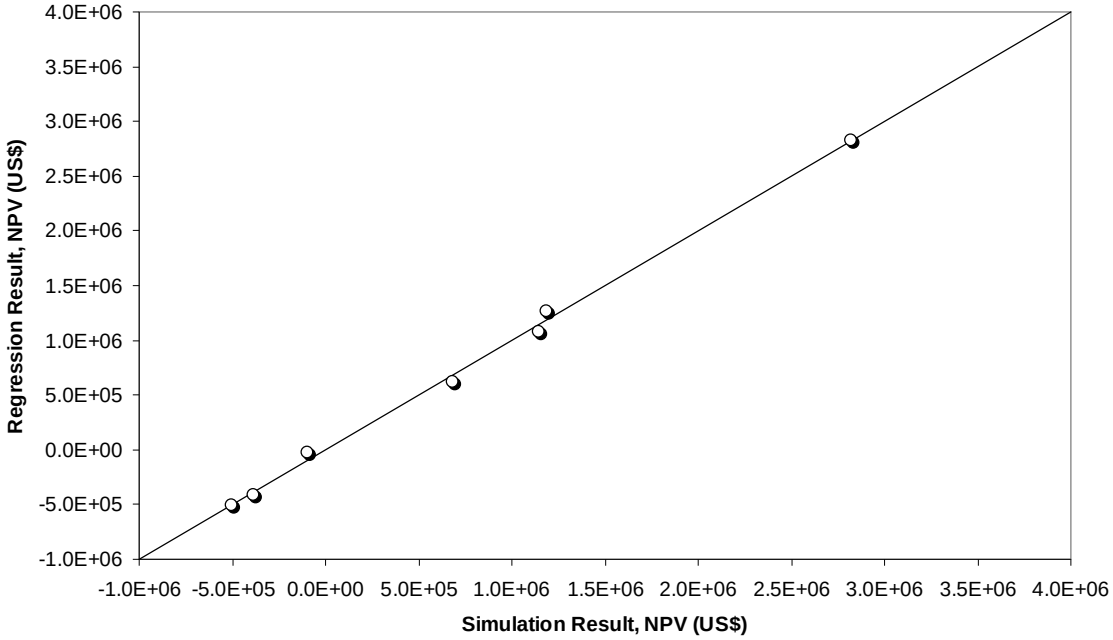

Fig. 4.5 - Regression model calibration for the One-Factor-A-Time method

Another regression model is built based on a "three factorial" design. A "three factorial" design has 3 values for each parameter. The values represent the extremities, which are the maximum, minimum, and most likely values.

This work uses a "three factorial design" of the Box Behnken method. While the Plackett-Burman method is mainly used as a screening tool to select the most influential factors, the Box Behnken method can be utilized as a tool to develop the regression of response from the simulation result.

Based on the screening result, the next sequence is to select the most important parameter that will be used in the regression model. Instead of using the Plackett-Burmann method, the Box Behnken method is chosen to conduct regression model. Both

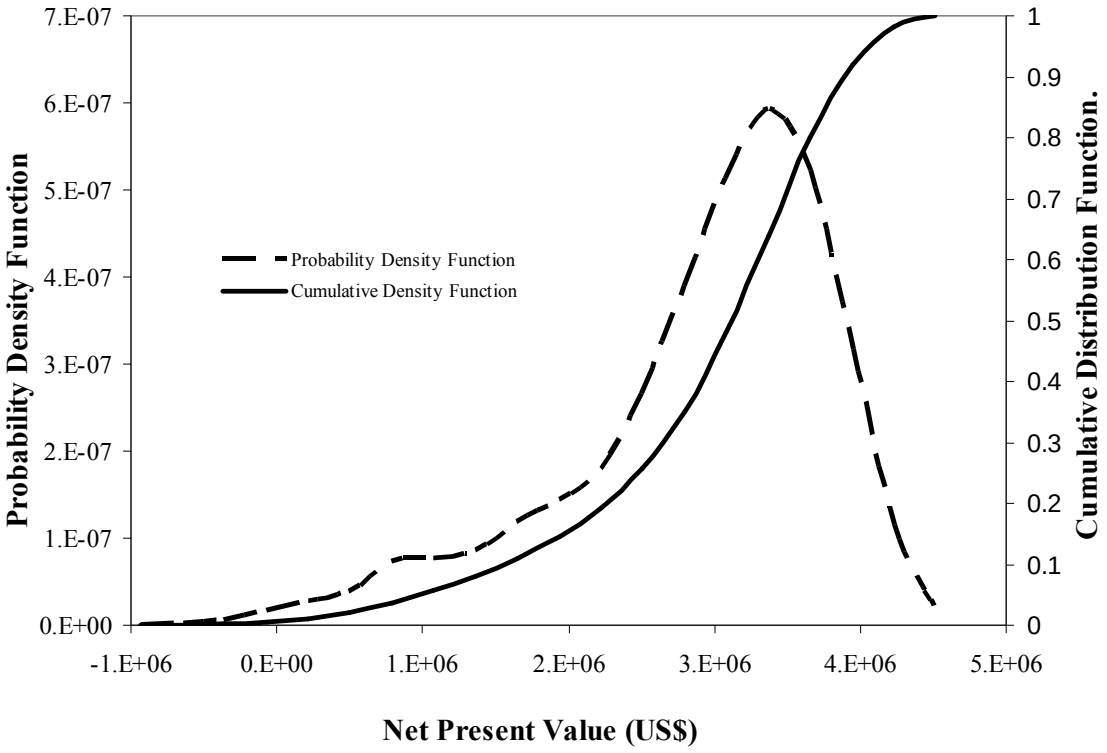

Fig. 4.6 - Probability density function and cumulative distribution function for the One-Factor-A-Time method

methods, the Plackett-Burman and Box Behnken, are condition-based probability. In condition-based probability, there are relationships among the factors. A number of simulation runs are designed based on the combinations among all factors in the minimum, most likely, and maximum values.

Table 4.5 - Data set for Box Behnken method				
Parameter	**Notation**	**Minimum**	**Most Likely**	**Maximum**
Fracture permeability, md	*F1*	0.1	1	50
Thickness, ft	*F2*	6.8	30	40
Langmuir volume, *gmole/lbm*	*F3*	0.06	0.23	0.4

Table 4.5 shows the range of 3 selected parameters that have been used in the Box Behnken method. This work used 16 simulation runs to provide regression model data. A detailed explanation of this method and the simulation runs result is available in Appendix E. The regression result for this method is:

$$NPV = -831267 - 338545\,F1 - 9345.5\,F2 + 9253000\,F3 + 1878000\sqrt{F1} + 259740\sqrt{F2} - 1735000\sqrt{F3} - 3401000\,e^{F3} + 1999.3\,F1F2 + 193907\,F1\sqrt{F3}$$

Based on the regression result, a graphical evaluation is shown in Fig. 4.7. The more the regression result matches with the 45-degree line, the better the regression result is.

The Net Present Value (NPV) is calculated from the cash flow in 20 years' gas production. Based on the selected regression model, this works used 10,000 random numbers in performing the Monte Carlo simulation. The Monte Carlo simulation provides the probability density function and cumulative density function of the Box Behnken method (Fig. 4.8).

A comparison of the One-Factor-A-Time method and the Box Behnken method is shown in Fig. 4.8. In this case, the Box Behnken method provides a more realistic probability and cumulative density function with a wider range. The Net Present Value range for the One-Factor-A-Time method is between US$ -931,970 and US$ 4,515,806. On the other hand, the Box Behnken method gives a broader range from US$ -5,086,248 to US$ 6,897,093. This result illustrates the main difference between the One-Factor-A-Time method and the Box Behnken method. The Box Behnken method, which is a factorial design, considers the extreme condition when there is relationship among factors.

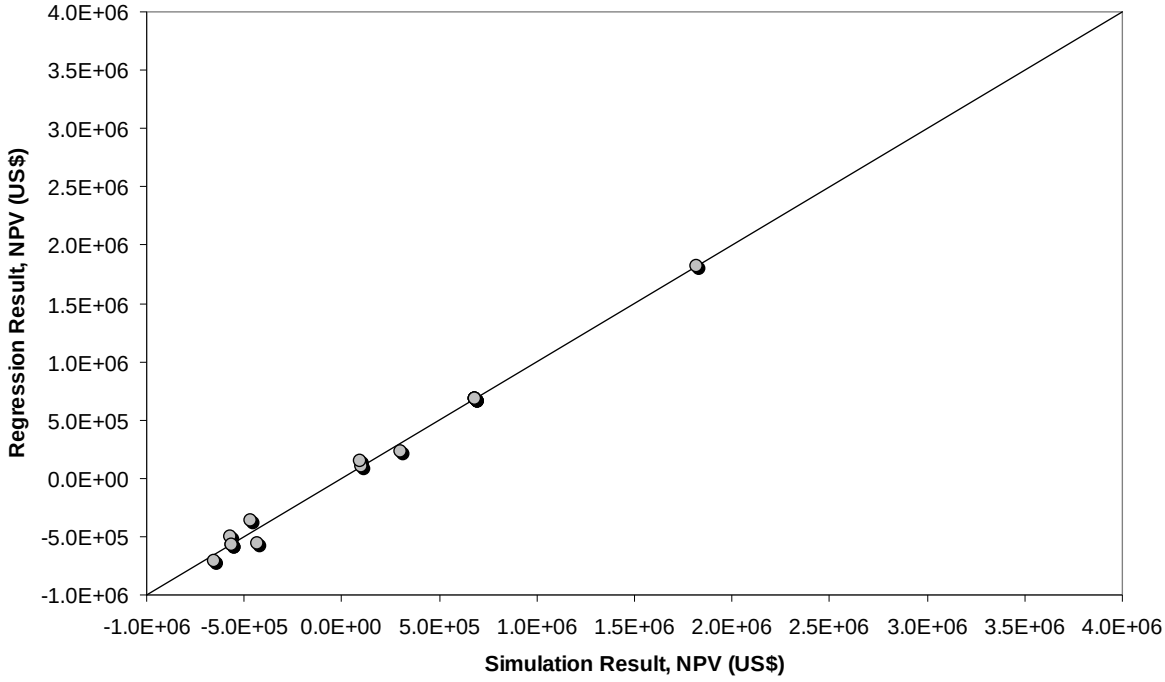

Fig. 4.7 - Regression model calibration for the Box Behnken method

Table 4.6 shows the Net Present Value comparison between the One-Factor-A-Time approach and the Box Behnken approach based on the Monte Carlo simulation result. The Monte Carlo simulation represents the uncertainty of the obtained Net Present Value model from the regression result of the sensitivity One-Factor-A-Time and Box Behnken methods. This work uses a triangle distribution to represent the uncertainty of each parameter.

To give better explanation, it is common to present the Monte Carlo simulation result with the following notations: P 10, P 50, and P 90. The meaning of the first notation (P 10) is the possibility to acquire a value lower than P 10 value is 10%. In other words, there is a possibility of 1 out of 10 that the outcome is lower than expected

value. The P 10 result is also known as the proved value. The same interpretation applies for P 50 and P 90 notations. The P 50 value is also known as the probable value and the P 90 as the possible value.

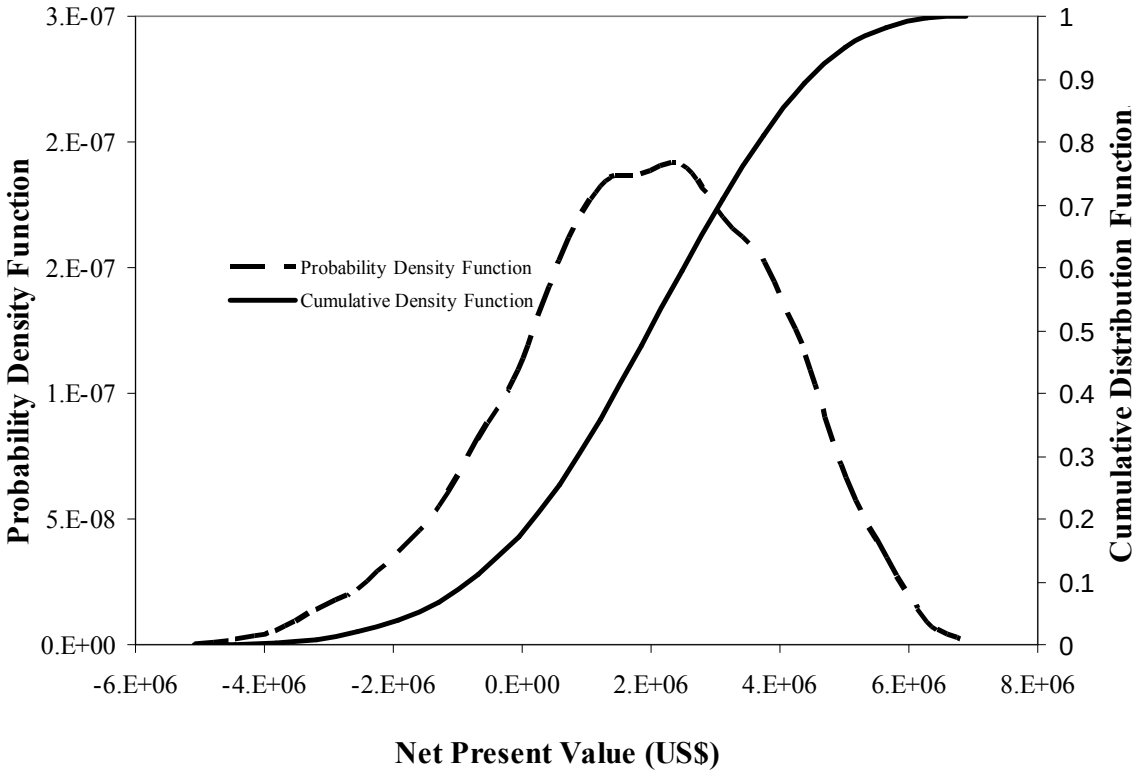

Fig. 4.8 - Probability density function and cumulative distribution function for the Box Behnken method

Table 4.6 - Net Present Value (US $)		
Parameter	**One Factor at A Time**	**Box Behnken**
P 10	1,559,034	-826,566
P 50	3,117,715	1,982,409
P 90	3,897,188	4,441,489
Minimum	-931,970	-5,086,248
Maximum	4,515,806	6,897,093

The Monte Carlo simulation needs a distribution type for the input data or parameters to present the uncertainty. The distribution type can be a normal distribution, a log normal distribution, a rectangle distribution, or a triangle distribution. This work uses a triangle distribution that can capture 3 values at a time: the minimum value, most-likely value, and maximum value.

By using parameters in a certain distribution type, regression model, and random number, one could yield a very different profile of distribution in the simulation result. A graphical approach has been used in this work as distribution function. As shown in Fig. 4.9, the probability density function and cumulative distribution function of the Box Behnken approach provide a wider Net Present Value range.

The Box Behnken method has been selected to perform the evaluation of well-spacing effect on an economic model. To investigate the effect of well spacing, this work has used the same data set and regression model. The similar work flow is applied to all well spacing scenarios (Fig. 4.10). The first step is to establish the simulation model. This step includes checking the consistency of the data set being used.

The following sequence is to identify the key responses from the simulation model. The key responses are the expected result from the simulation model; it could be a recovery factor, cumulative gas production, or original gas in place. Afterwards, the next sequence is to identify parameters in the input data and the uncertainty ranges.

The next step is to run simulation using extreme cases to check the stability of the simulation model in extreme conditions. The next step is to perform a parametric study to screen the most influential factors that will be used in regression model. In this

step, a modification of range parameter is required in each case that yields an unstable simulation result.

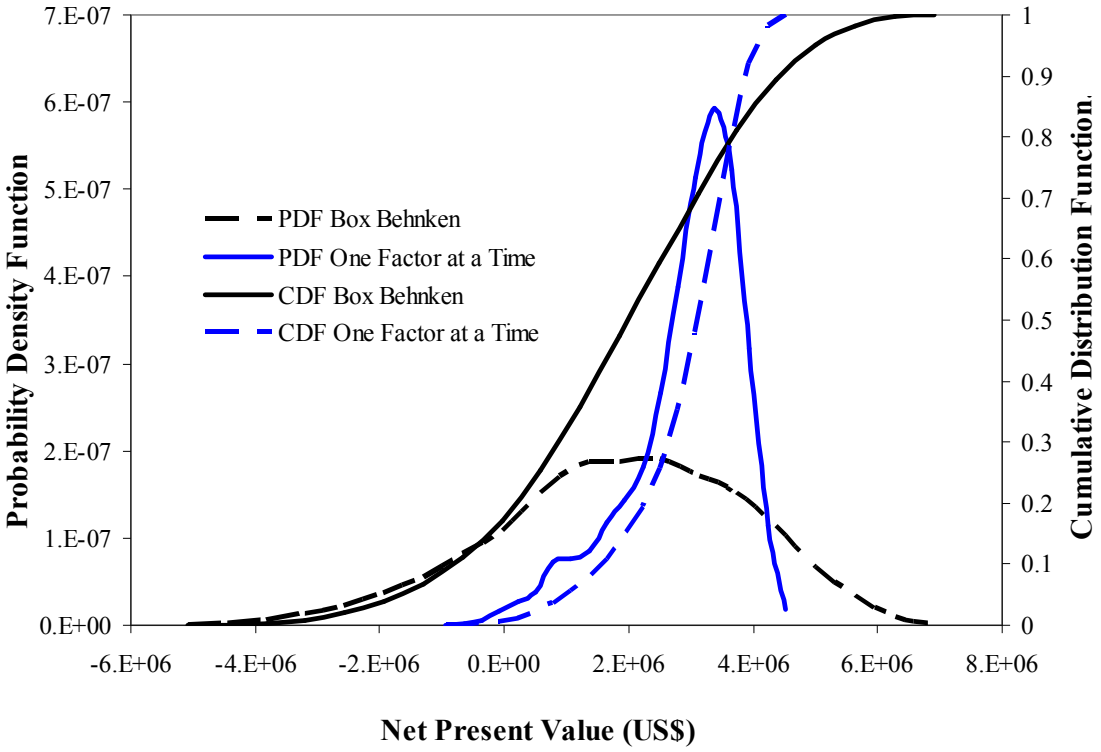

Fig. 4.9 - Comparison of probability density function and cumulative distribution function

After selecting the most influential factors that will be used in the regression model, then the regression model can be initiated. The regression model result needs to be evaluated whether it is consistent with the reservoir simulation result. This step can be done by using a graphical approach plotting regression model result and a simulation model result. If the regression result is acceptable, the plot will tend to follow the 45-degree tangent line.

When the regression result is not agreeable, a trial and error approach in building the regression model is necessary. If the regression model is found satisfying, the next step is to perform the Monte Carlo simulation. Before conducting the Monte Carlo simulation, one should establish the distribution of the input parameter. This work has used a triangle distribution to present uncertainty of response function. The response function in this model is the Net Present Value per acre after having 20 years of production.

As shown in Fig. 4.11, each well-spacing scenario alters the probability distribution function and cumulative distribution function of the Net Present Value (calculated per acre for 20 years' production). A better economic model result tends to shift the curve to the right. Following each pair of curves (the probability density function and cumulative density function), the 320-acre well-spacing creates the lowest Net Present Value distribution.

Furthermore, decreasing well-spacing seems to improve the Net Present Value distribution. However, there is an optimum condition between 40 acres and 80 acres. Increasing well-spacing to 320 acres tends to shift the Net Present Value distribution function to the left as shown in Fig. 4.11. It means well-spacing scenarios bigger than 80 acres creates a lower Net Present Value distribution.

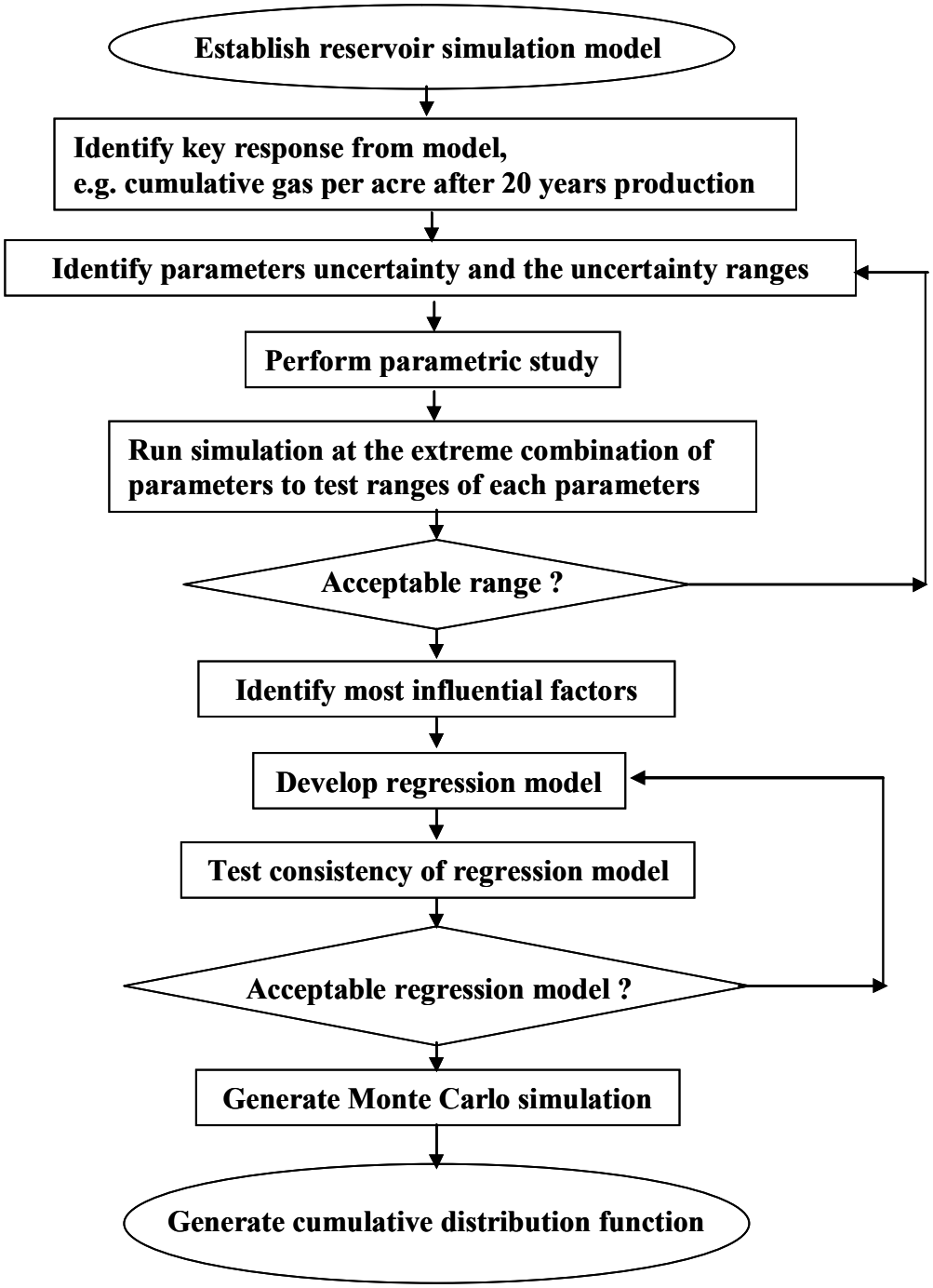

Fig. 4.10 – Well-spacing study work flow

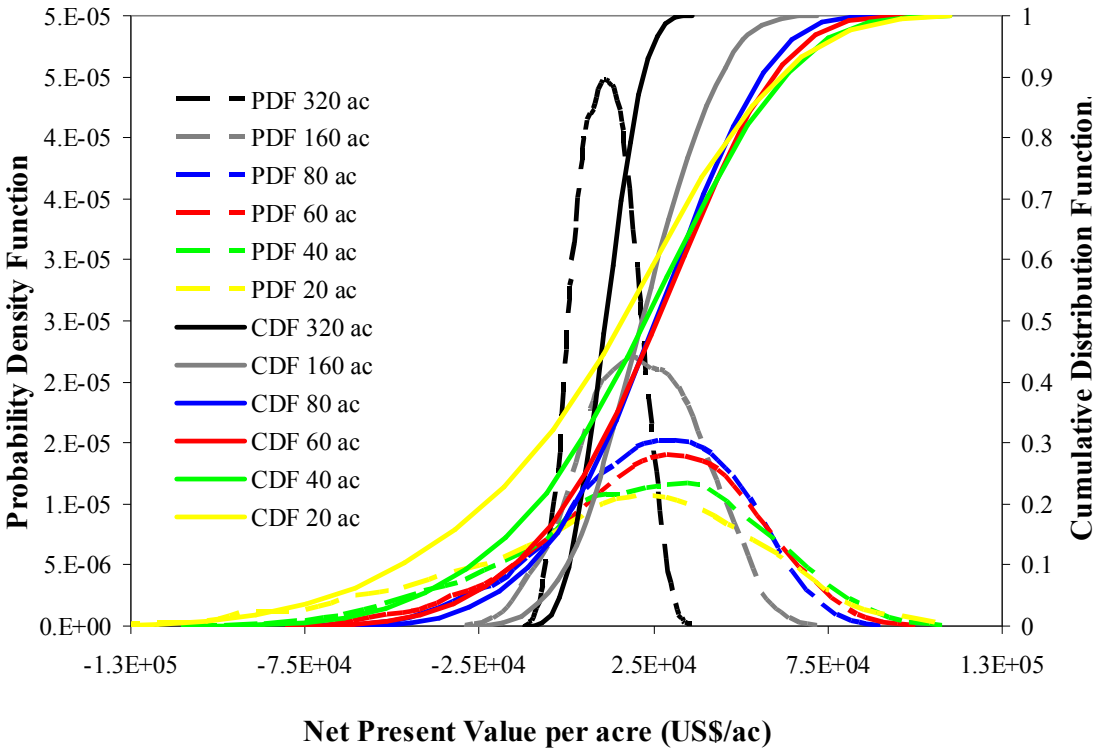

Fig. 4.11 - Comparison of distribution function

CHAPTER V

CONCLUSIONS AND RECOMMENDATIONS

5.1 Conclusions

Based on the obtained results of this research, I offer the following conclusions:

1) To perform reservoir simulation, it is necessary to investigate the consistency of the reservoir model result. In a special case, the combination of each parameter in a coalbed methane reservoir model can yield inconsistency in the numerical model result.
2) A parametric study is mandatory in evaluating the uncertainty of reservoir properties. A parametric study gives illustration about the relationship among the parameters and provides possible extreme conditions that should be considered in coalbed methane reservoir modeling.
3) As a screening technique, the Placket-Burman method can be utilized to investigate the influence of each parameter based on the various possible combinations with other parameters.
4) A regression model needs a “three factorial design” to present the minimum, most likely, and maximum condition of each parameter. The Box Behnken method provides an approach to model the response of reservoir simulation results. This method can be used in building a regression model to replace reservoir simulation using the Monte Carlo simulation.

5) Investigation of well-pacing effect can be conducted using the Monte Carlo simulation as a representative of the uncertainty in the reservoir properties.

5.2 Recommendations

The following recommendations are proposed to improve a well-spacing study in a coalbed methane reservoir:

1. It is necessary to build an interface application between input data modification (excel file) and reservoir simulator (CMG). By using this application one could perform simulation runs without making data input for each case, and so a wider parametric study can be done automatically. Another advantage of having this application is that it can avoid human errors in finding the result of the simulation run and in entering input data for the simulator.
2. It is necessary to continue a well-spacing study with different reservoir models. For instance, researchers should investigate hydraulic fracturing and its effect on well-spacing scenarios. The study can also include investigation of a hydraulic fracturing model with different half-lengths and conductivities. The study can also be improved by considering horizontal wells for a thin formation. Another variable in the horizontal well model is the horizontal length. This variable should be incorporated in the regression model.
3. The dewatering phase in a coalbed methane reservoir needs to be investigated. A further study can be conducted based on aquifer modeling and its influence on well-spacing study.

NOMENCLATURE

q = drainage rate per unit volume,

p = pressure, psia

B = formation volume factor, rb/stb

S = saturation, fraction

r = radius, ft

t = time, days

C = Coalbed gas content, Mscf/rcf

F_s = shape factor, 1/ft^2

D = Diffusion coefficient, cm^2/sec

D_c = diffusion coefficient, ft^2/day

A = area, ft^2

k = permeability, md

L = Length, ft

$V(p)$ = gas content a pressure = p, scf/ton

V_L = Langmuir volume, scf/ton

p_L = Langmuir pressure, psia

Greek symbols

μ = viscosity, cp

ϕ = porosity

ω = dimensionless storativity ratio

σ = shape factor, ft^{-2}

λ = dimensionless interporosity flow parameter

τ = sorption time, days

Subscript

w = *water*

g = gas

m = matrix

f = fracture

REFERENCES

1. Annual Energy Outlook 2010, U.S. Energy Information Administration. DOE/EIA-0383(2010). http://www.eia.doe.gov/oiaf/aeo/pdf/0383(2010).pdf
2. International Energy Outlook 2010, U.S. Energy Information Administration, DOE/EIA-0484(2010). http://www.eia.doe.gov/oiaf/ieo/pdf/0484(2010).pdf
3. Ayers Jr., W. B. 2002. Coalbed Gas Systems, Resources, and Production and a Review of Contrasting Cases from the San Juan and Powder River Basins. *AAPG Bulletin*. **86:** 1853-1890.
4. Ayers, W. B. Fall 2008. PETE 612 – Unconventional Reservoir Class Notes, Texas A&M University.
5. Cook, T. 2005. Chapter 23: Calculation of Estimated Ultimate Recovery (EUR) for Wells in Continuous Type Oil and Gas Accumulations. www.pubs.usgs.gov /dds/dds-069/dds-069-d/REPORTS/69_D_CH_23.pdf
6. Wise, R.L. 1979. Methane Recovery and Utilization from Coalbeds. SPE-8357.
7. John, Mike, Paul, Andrew, Charles, *et al*.2003. Producing Natural Gas from Coal. *Oilfield Review*, **Autumn 2003**: 8-31.
8. Warren, J.E., and Root, P.J. 1963. The Behavior of Naturally Fractured Reservoirs. SPE-426..
9. Puri, R., and Yee, D. 1990. Enhanced Coalbed Methane Recovery. SPE-20732.

10. Barenblatt, G.I., Zheltov, I. P., and Kochina, I.N. 1960. Basic Concepts in the Theory of Seepage of Homogeneous Liquids in Fissured Rocks (Strata). *PMM*. **24 No 5**: 852-864.
11. David, Turgay, Wonmo, and Gregory. 1984. A Parametric Study of the Effects of Coal Seam Properties on Gas Drainage Efficiency. SPE-13366.
12. Olufemi, Turgai, Duane, Grant, Neal, *et al*. 2004. Carbon Dioxide Sequestration in Coal Seams: A Parametric Study and Development of a Practical Prediction/Screening Tool Using Neuro-Simulation. SPE-90055.
13. Cervik, J.1967. Behavior of Coal-Gas Reservoir. SPE-1973.
14. Zuber, M.D., Sawyer, W.K., Schraufnagel, R.A., and Kuuskaraa, V.A. 1987. The Use of Simulation and History Matching to Determine Critical Coalbed Methane Reservoir Properties. SPE-16420.
15. Seidle, J.P. and Arri, L.E. 1990. Use of Conventional Reservoir Models for Coalbed Methane Simulation. SPE-21599.
16. King, G.R. 1990. Material Balance Techniques for Coal Seam and Devonian Shale Gas Reservoirs. SPE-20730.
17. Seidle J.P. 1999. A Modified p/z Method for Coal Wells. SPE-55605.
18. David, H. and Law, S. 2002. Numerical Simulator Comparison Study for Enhanced Coalbed Methane Recovery Processes, Part I: Carbon Dioxide Injection. SPE-75669.
19. Hower, T.L.2003. Coalbed Methane Reservoir Simulation: An Evolving Science. SPE-84424.

20. Jalal, J. and Shahab, D.M. 2004. A Coalbed Methane Reservoir Simulator Designed for the Independent Producers. SPE-91414.

21. Aminian, K., Ameri, S., Bhavsar, A., Sanchez, M., and Garcia, A. Type Curves for Coalbed Methane Production Prediction. SPE-91482.

22. Reeves, S. and Pekot, L. 2001. Advanced Reservoir Modeling in Desorption-Controlled Reservoirs. SPE-71090.

23. Thomas, Tan. 2002. Advanced Large–Scale Coalbed Methane Modeling Using a Conventional Reservoir Simulator. SPE-75672.

24. Paul, G.W., Sawyer, W.K., and Dean, R.H. 1990. Validation of 3D Coalbed Simulators. SPE-20733.

25. Xiao Guo, Zhimin Du, and Shilun Li. 2003. Computer Modeling and Simulation of Coalbed Methane Reservoir. SPE-84815.

26. Derickson, J.P., Horne, J.S., Fisher, R.D., and Stevens, S.H. 1998. Huabei Coalbed Methane Project, Anhui Province, People's Republic of China. SPE-48886.

27. Roadifer, R.D., Moore, T.R., Raterman, K.T., Farnan, R.A., and Crabtree, B.J. Coalbed Methane Parametric Study: What's Really Important to Production and When?. SPE-84425.

28. Stevenson, M.D., Pinczewski, W.V., and Downey, R.A. 1993. Economic Evaluation of Nitrogen Injection for Coalseam Gas Recovery. SPE-26199.

29. Reeves, S.R. and Decker, A.D.1991. A Reservoir Simulation Investigation into the Interaction of Is-Situ Stress, Pore Pressure, and Coal Rank on Coalbed Methane Exploration Strategy. SPE-21490.

30. Young, G.B.C., McElhiney, J.E., Paul, G.W., and McBane, R.A. 1991. An Analysis of Fruitland Coalbed Methane Production, Cedar Hill Field, Northern San Juan Basin. SPE-22913.

31. Young, G.B.C., McElhiney, J.E., Paul, G.W., and McBane, R.A.1992. A Parametric Analysis of Fruitland Coalbed Methane Producibility. SPE-24903.

32. Wicks, D.E., Schewerer, F. C., Militzer, M.R., and Zuber, M.D. 1986. Effective Production Strategies for Coalbed Methane in the Warrior Basin. SPE-15234.

33. Chaianansutcharit, T. Her-Yuan Chen, and Teufel, L.W. 2001. Impacts of Permeability Anisotropy and Pressure Interference on Coalbed Methane (CBM) Production. SPE-71069..

34. King, G.R. 1990. Material-Balance Techniques for Coal Seam and Devonian Shale Gas Reservoirs with Limited Water Influx. SPE-20730.

35. Jochen, V.A., Lee, W.J., and Semmelback, M.E. 1994. Determining Permeability in Coalbed Methane Reservoirs. SPE-28584.

36. Reservoir Assesment Report Analysis Submitted to El Paso Production Company, Ticora Geo., Arvada, Colorado, (August 2004).

37. Kohler, E.T. and Ertekin, Turgay. 1995. Modeling of Undersaturated Coal Seam Gas Reservoirs. SPE-29578.

38. Bumb, A.C. and McKee, C.R. 1984. Use of a Computer Model to Design Optimal Well for Dewatering Coal Seams for Methane Production. SPE-12859.

39. Sung, W., Ertekin, T., and Schewerer, F. C. 1987. An Analysis of Field Development Strategies for Methane Production from Coal Seams. SPE-16858.

40. CMG; GEM 2003.10 User Guide, Computer Modeling Group Calgary, Canada.

41. Kamel Rekab and Muzaffar Shaikh. Statistical Design of Experiments with Engineering Applications. CRC Press, 2005

APPENDIX A

CMG BASE CASE DATA FILE

```
*TITLE1 'CBM Case'
*INUNIT *FIELD
*INTERRUPT *INTERACTIVE
*XDR *ON
*OUTSRF *WELL
*MAXERROR 20
*RANGECHECK ON
*WRST  0
*WPRN *WELL 5
*WPRN *GRID *TIME
*WSRF *WELL 5
*WSRF *GRID 1
*OUTPRN *WELL *ALL
*OUTPRN *GRID *PRES *SW *SG *DENW *DENG *VISG  *ADS 'C1' *Y 'C1'
*OUTPRN *RES  *ALL
*OUTSRF *GRID *PRES *SW *SG *DENW *DENG *VISG  *ADS 'C1' *Y 'C1'
*OUTSRF *RES  *ALL


**-------------------------------------------------RESERVOIR DATA------
*GRID *RADIAL 31 1 1 *RW   1.5
*KDIR *DOWN
*DI *IVAR
0.353   0.436   0.539   0.666
        0.823   1.016   1.256
        1.551   1.917   2.368
        2.925   3.614   4.465
        5.516   6.815   8.419
        10.401 12.850 15.875
        19.613 24.231 29.935
        36.983 45.690 56.448
        69.737 86.156 150.277
        150.277         150.277
        150.277
*DJ *CON 360
*DK *CON  30
*PAYDEPTH *ALL 31*3280
```

```
**----------------------------------------DUAL POROSSITY OPTION-----
*DUALPOR
*NULL *MATRIX *CON 1.
*NULL *FRACTURE *CON 1.
*PINCHOUTARRAY *CON 1.

**----------------------------------------POROSITY DATA-------------
*POR *MATRIX *CON 0.005
*POR *FRACTURE *CON 0.001

**----------------------------------------PERMEABILITY DATA---------
*PERMI *MATRIX   *CON 0.00001
*PERMI *FRACTURE *CON 1
*PERMJ *MATRIX   *CON 0.00001
*PERMJ *FRACTURE *CON 1
*PERMK *MATRIX   *CON 0.00001
*PERMK *FRACTURE *CON 1

**--------------------------------------FRACTURE SPACING DATA----------
*DIFRAC *CON  0.042
*DJFRAC *CON  0.042
*DKFRAC *CON  0.042
*-------------------------------------COMPRESSIBILITY DATA (MATRIX)--
*CPOR *MATRIX 100E-6
*PRPOR *MATRIX 1109.54
**------------------------------------COMPRESSIBILITY DATA (FRACTURE)--
*CPOR *FRACTURE 100E-6
*PRPOR *FRACTURE 1109.54
**-----------------------------METHANE AND WATER DATA-----------------
*MODEL   *PR
*NC    1    1
*COMPNAME 'C1'
*HCFLAG    0
*VISCOR *HZYT
*VISCOEFF   0.1023
          0.023364
          0.058533
          -0.040758
          0.0093324
*MIXVC      1
*TRES       113. **F
*PCRIT      45.4
*TCRIT      190.6
*AC         0.008
```

```
*VCRIT      0.099
*MW         16.043
*PCHOR      77
*SG         0.3
*TB         -258.61
*VISVC      0.099
*VSHIFT     0
*OMEGA      0.45723553
*OMEGB      0.077796074
*PVC3       1.2
*PHASEID *DEN
*DENW       62.4
*CW         3.99896E-06
*REFPW      14.69595
*VISW       0.607
**======================== ROCK-FLUID PROPERTIES
*ROCKFLUID
** GAS COAL NATURAL FRACTURE REL. PERM WATER-GAS
*RPT 1
*SWT
**   Sw        Krw       Krow
** -------    --------    --------
  0.00000     0.0000     1.0
  1.00000     1.0000     0.0
*SGT
** Gas Sat    Krg       Krog
** -------    --------    --------
  0.0          0.0          1.0
  1.0          1.0          0.0
** Use the same relperm for matrix and fractures
*RPT 2
*SWT
**   Sw        Krw       Krow
** -------    --------    --------
  0.00000     0.0000     1.0
  1.00000     1.0000     0.0
*SGT
** Gas Sat    Krg       Krog
** -------    --------    --------
  0.0          0.0          1.0
  1.0          1.0          0.0
*RTYPE MATRIX   CON 1
*RTYPE FRACTURE CON 2
```

```
**------------ SORPTION ISOTHERM DATA------------------
*ROCKDEN MATRIX   CON 89.58 **(lb/ft3)** Matrix & fracture density, specific
gravity * 62.428
*ROCKDEN FRACTURE CON 89.58  **(lb/ft3)
** NO SORPTION IN FRACTURE SYSTEM
** IN-SITU LANGMUIR STORAGE CAPACITY, gmole/lb
*ADGMAXC 'C1' FRACTURE CON 0.0
** RECIPROCAL LANGMUIR PRESSURE, 1/psi
*ADGCSTC 'C1' FRACTURE CON 0.0
** SORPTION IN MATRIX
** IN-SITU LANGMUIR STORAGE CAPACITY gmole / lbm
** g mole / lbm rock = 5.9760E-4 * scf/ton
*ADGMAXC 'C1' MATRIX CON 0.23
** RECIPROCAL LANGMUIR PRESSURE, 1/psi
*ADGCSTC 'C1' MATRIX CON   0.0014
 ** Coal Sorption times, Days
*COAL-DIF-TIME 'C1' CON 10

**-------------------------------------------------INITIAL CONDITION-------
*INITIAL
*VERTICAL  *BLOCK_CENTER *COMP
*NREGIONS  2
REFPRES
  1109.54 1109.54
REFDEPTH
  3280  3280
DWOC
  328  328
SWOC
  0.9999  0.592
CDEPTH
  3280  3280
ZDEPTH
 1 3280 1
 2 3280 1
*SEPARATOR 14.69595   59
*ITYPE *MATRIX *CON 2.
*ITYPE *FRACTURE *CON 1.

**-------------------------------------------------NUMERICAL DATA----------
*NUMERICAL
DTMAX 30
CONVERGE PRESS 0.514884
*RUN
```

```
**----------------------------------------------SIMULATION---------------
**START DATE
*DATE 2000 01 01
** **-----------------------------------------------WELL DATA---------------
** *WELL 1   'PRODUCER 1'
**$
WELL  'PRODUCER 1'
**-------------------------------------------PRODUCTION CONSTRAINT--------
PRODUCER 'PRODUCER 1'
OPERATE  MIN  BHP  14.7  CONT
**$         rad  geofac  wfrac  skin
GEOMETRY  K  0.25  0.37  1.  3.
PERF  GEO  'PRODUCER 1'
**$ UBA    ff  Status  Connection
   1 1 1  1.  OPEN    FLOW-TO  'SURFACE'
**$ RESULTS PROP AIMSET FRACTURE Units: Dimensionless
**$ RESULTS PROP Minimum Value: 3 Maximum Value: 3
*AIMSET *FRACTURE *CON 3
**$ RESULTS PROP AIMSET MATRIX Units: Dimensionless
**$ RESULTS PROP Minimum Value: 3 Maximum Value: 3
*AIMSET *MATRIX   *CON 3
**-----------------------------------------TIME STEP--------------------
*TIME1
*TIME2
*TIME10
*TIME20
*TIME30
cont.
*TIME7280
*TIME7300
STOP
**---------------------------------------TERMINATE SIMULATION-----------
```

APPENDIX B

ONE-FACTOR-AT-A-TIME METHOD CALCULATION

Table 4.2- Parameter range				
Parameter	**Min**	**Base**	**Max**	**Notation**
Thickness, *ft*	6.8	30	40	***F1***
Matrix porosity, *fraction*	0.0025	0.005	0.04	***F2***
Fracture porosity, *fraction*	0.0025	0.003	0.3	***F3***
Matrix permeability, *md*	0.01	0.1	1000	***F4***
Fracture permeability, *md*	0.1	1	50	***F5***
Fracture cleat spacing, *ft*	0.017	0.042	0.05	***F6***
Matrix compressibility, 10^{-6} *psi-1*	10	100	200	***F7***
Fracture compressibility, 10^{-6} *psi-1*	10	100	200	***F8***
Water density. lb/ft^3	62.4	62.4	62.7	***F9***
Water compressibility, psi^{-1}	2E-06	3E-06	4E-06	***F10***
Water viscosity, *cp*	0.550	0.607	0.730	***F11***
Reservoir temperature, *°F*	68	113	114	***F12***
Coal density, lb/ft^3	81.00	89.58	109	***F13***
Langmuir volume, *gmole/lbm*	0.06	0.23	0.4	***F14***
Reciprocal Langmuir pressure, psi^{-1}	0.001	0.0014	0.0032	***F15***
Desorption time, *Days*	5	10	20	***F16***
Initial pressure, *psi*	339	1110	1422	***F17***
Initial water saturation, *Fracture*	0.77	0.999	1	***F18***
Initial water saturation, *Matrix*	0.1	0.592	1	***F19***
Skin	-6	0	6	***F20***

Table B.2 - One factor at a time simulation result

		Simulation Run				
		1	**2**	**3**	**4**	**5**
Parameter	**F1**	30	6.8	40	30	30
	F2	0.005	0.005	0.005	0.0025	0.04
	F3	0.003	0.003	0.003	0.003	0.003
	F4	0.1	0.1	0.1	0.1	0.1
	F5	1	1	1	1	1
	F6	0.042	0.042	0.042	0.042	0.042
	F7	100	100	100	100	100
	F8	100	100	100	100	100
	F9	62.4	62.4	62.4	62.4	62.4
	F10	3E-06	3E-06	3E-06	3E-06	3E-06
	F11	0.607	0.607	0.607	0.607	0.607
	F12	113	113	113	113	113
	F13	89.5841	89.5841	89.5841	89.5841	89.5841
	F14	0.23	0.23	0.23	0.23	0.23
	F15	0.00138	0.00138	0.00138	0.00138	0.00138
	F16	10	10	10	10	10
	F17	1109.54	1109.54	1109.54	1109.54	1109.54
	F18	0.999	0.999	0.999	0.999	0.999
	F19	0.592	0.592	0.592	0.592	0.592
	F20	0	0	0	0	0
	Response, *MMscf/acre*	8.182	1.855	10.909	8.031	10.233
		Simulation Run				
		6	**7**	**8**	**9**	**10**
Parameter	**F1**	30	30	30	30	30
	F2	0.005	0.005	0.005	0.005	0.005
	F3	0.0025	0.3	0.003	0.003	0.003
	F4	0.1	0.1	0.01	1000	0.1
	F5	1	1	1	1	0.1
	F6	0.042	0.042	0.042	0.042	0.042
	F7	100	100	100	100	100
	F8	100	100	100	100	100
	F9	62.4	62.4	62.4	62.4	62.4
	F10	3E-06	3E-06	3E-06	3E-06	3E-06
	F11	0.607	0.607	0.607	0.607	0.607
	F12	113	113	113	113	113
	F13	89.5841	89.5841	89.5841	89.5841	89.5841
	F14	0.23	0.23	0.23	0.23	0.23
	F15	0.00138	0.00138	0.00138	0.00138	0.00138
	F16	10	10	10	10	10
	F17	1109.54	1109.54	1109.54	1109.54	1109.54
	F18	0.999	0.999	0.999	0.999	0.999
	F19	0.592	0.592	0.592	0.592	0.592
	F20	0	0	0	0	0
	Response, *MMscf/acre*	8.296	0.837	8.182	8.182	1.662

Table B.2 - One factor at a time simulation result

		Simulation Run				
		11	**12**	**13**	**14**	**15**
Parameter	**F1**	30	30	30	30	30
	F2	0.005	0.005	0.005	0.005	0.005
	F3	0.003	0.003	0.003	0.003	0.003
	F4	0.1	0.1	0.1	0.1	0.1
	F5	50	1	1	1	1
	F6	0.042	0.017	0.05	0.042	0.042
	F7	100	100	100	10	200
	F8	100	100	100	100	100
	F9	62.4	62.4	62.4	62.4	62.4
	F10	3E-06	3E-06	3E-06	3E-06	3E-06
	F11	0.607	0.607	0.607	0.607	0.607
	F12	113	113	113	113	113
	F13	89.5841	89.5841	89.5841	89.5841	89.5841
	F14	0.23	0.23	0.23	0.23	0.23
	F15	0.00138	0.00138	0.00138	0.00138	0.00138
	F16	10	10	10	10	10
	F17	1109.54	1109.54	1109.54	1109.54	1109.54
	F18	0.999	0.999	0.999	0.999	0.999
	F19	0.592	0.592	0.592	0.592	0.592
	F20	0	0	0	0	0
	Response, *MMscf/acre*	13.500	8.182	8.182	8.175	8.190
		Simulation Run				
		16	**17**	**18**	**19**	**20**
Parameter	**F1**	30	30	30	30	30
	F2	0.005	0.005	0.005	0.005	0.005
	F3	0.003	0.003	0.003	0.003	0.003
	F4	0.1	0.1	0.1	0.1	0.1
	F5	1	1	1	1	1
	F6	0.042	0.042	0.042	0.042	0.042
	F7	100	100	100	100	100
	F8	10	200	100	100	100
	F9	62.4	62.4	62.4	62.712	62.4
	F10	3E-06	3E-06	3E-06	3E-06	2E-06
	F11	0.607	0.607	0.607	0.607	0.607
	F12	113	113	113	113	113
	F13	89.5841	89.5841	89.5841	89.5841	89.5841
	F14	0.23	0.23	0.23	0.23	0.23
	F15	0.00138	0.00138	0.00138	0.00138	0.00138
	F16	10	10	10	10	10
	F17	1109.54	1109.54	1109.54	1109.54	1109.54
	F18	0.999	0.999	0.999	0.999	0.999
	F19	0.592	0.592	0.592	0.592	0.592
	F20	0	0	0	0	0
	Response, *MMscf/acre*	8.182	8.183	8.182	8.182	8.182

Table B.2 - One factor at a time simulation result

		Simulation Run				
		21	**22**	**23**	**24**	**25**
Parameter	**F1**	30	30	30	30	30
	F2	0.005	0.005	0.005	0.005	0.005
	F3	0.003	0.003	0.003	0.003	0.003
	F4	0.1	0.1	0.1	0.1	0.1
	F5	1	1	1	1	1
	F6	0.042	0.042	0.042	0.042	0.042
	F7	100	100	100	100	100
	F8	100	100	100	100	100
	F9	62.4	62.4	62.4	62.4	62.4
	F10	4E-06	3E-06	3E-06	3E-06	3E-06
	F11	0.607	0.55	0.73	0.607	0.607
	F12	113	113	113	68	114
	F13	89.5841	89.5841	89.5841	89.5841	89.5841
	F14	0.23	0.23	0.23	0.23	0.23
	F15	0.00138	0.00138	0.00138	0.00138	0.00138
	F16	10	10	10	10	10
	F17	1109.54	1109.54	1109.54	1109.54	1109.54
	F18	0.999	0.999	0.999	0.999	0.999
	F19	0.592	0.592	0.592	0.592	0.592
	F20	0	0	0	0	0
	Response, *MMscf/acre*	8.182	8.238	8.067	8.579	8.174
		Simulation Run				
		26	**27**	**28**	**29**	**30**
Parameter	**F1**	30	30	30	30	30
	F2	0.005	0.005	0.005	0.005	0.005
	F3	0.003	0.003	0.003	0.003	0.003
	F4	0.1	0.1	0.1	0.1	0.1
	F5	1	1	1	1	1
	F6	0.042	0.042	0.042	0.042	0.042
	F7	100	100	100	100	100
	F8	100	100	100	100	100
	F9	62.4	62.4	62.4	62.4	62.4
	F10	3E-06	3E-06	3E-06	3E-06	3E-06
	F11	0.607	0.607	0.607	0.607	0.607
	F12	113	113	113	113	113
	F13	81	109	89.5841	89.5841	89.5841
	F14	0.23	0.23	0.06	0.4	0.23
	F15	0.00138	0.00138	0.00138	0.00138	0.001
	F16	10	10	10	10	10
	F17	1109.54	1109.54	1109.54	1109.54	1109.54
	F18	0.999	0.999	0.999	0.999	0.999
	F19	0.592	0.592	0.592	0.592	0.592
	F20	0	0	0	0	0
	Response, *MMscf/acre*	7.629	9.356	3.111	11.840	7.897

Table B.2 - One factor at a time simulation result

		Simulation Run					
		31	**32**	**33**	**34**	**35**	
Parameter	**F1**	30	30	30	30	30	
	F2	0.005	0.005	0.005	0.005	0.005	
	F3	0.003	0.003	0.003	0.003	0.003	
	F4	0.1	0.1	0.1	0.1	0.1	
	F5	1	1	1	1	1	
	F6	0.042	0.042	0.042	0.042	0.042	
	F7	100	100	100	100	100	
	F8	100	100	100	100	100	
	F9	62.4	62.4	62.4	62.4	62.4	
	F10	3E-06	3E-06	3E-06	3E-06	3E-06	
	F11	0.607	0.607	0.607	0.607	0.607	
	F12	113	113	113	113	113	
	F13	89.5841	89.5841	89.5841	89.5841	89.5841	
	F14	0.23	0.23	0.23	0.23	0.23	
	F15	0.0032	0.00138	0.00138	0.00138	0.00138	
	F16	10	5	20	10	10	
	F17	1109.54	1109.54	1109.54	339	1422	
	F18	0.999	0.999	0.999	0.999	0.999	
	F19	0.592	0.592	0.592	0.592	0.592	
	F20	0	0	0	0	0	
	Response, *MMscf/acre*	7.658	8.187	8.172	2.166	9.619	

		Simulation Run					
		36	**37**	**38**	**39**	**40**	**41**
Parameter	**F1**	30	30	30	30	30	30
	F2	0.005	0.005	0.005	0.005	0.005	0.005
	F3	0.003	0.003	0.003	0.003	0.003	0.003
	F4	0.1	0.1	0.1	0.1	0.1	0.1
	F5	1	1	1	1	1	1
	F6	0.042	0.042	0.042	0.042	0.042	0.042
	F7	100	100	100	100	100	100
	F8	100	100	100	100	100	100
	F9	62.4	62.4	62.4	62.4	62.4	62.4
	F10	3E-06	3E-06	3E-06	3E-06	3E-06	3E-06
	F11	0.607	0.607	0.607	0.607	0.607	0.607
	F12	113	113	113	113	113	113
	F13	89.5841	89.5841	89.5841	89.5841	89.5841	89.5841
	F14	0.23	0.23	0.23	0.23	0.23	0.23
	F15	0.00138	0.00138	0.00138	0.00138	0.00138	0.00138
	F16	10	10	10	10	10	10
	F17	1109.54	1109.54	1109.54	1109.54	1109.54	1109.54
	F18	0.77	1	0.999	0.999	0.999	0.999
	F19	0.592	0.592	0.1	1	0.592	0.592
	F20	0	0	0	0	0	6
	Response, *MMscf/acre*	8.351	8.182	8.182	8.182	8.182	6.692

Table B.3 - Main effect result	
Parameter	**Response**
Fracture permeability, *md*	11.8383
Thickness, *ft*	9.0546
Langmuir volume, *gmole/lbm*	8.7288
Initial pressure, *psi*	7.8728
Fracture porosity, *fraction*	7.4588
Matrix porosity, *fraction*	2.2023
Water viscosity, *cp*	1.7273
Skin	1.4900
Coal density, lb/ft^3	0.4055
Reciprocal Langmuir pressure, psi^{-1}	0.2391
Reservoir temperature, *°F*	0.1704
Initial water saturation, Fracture	0.1694
Matrix compressibility, 10^{-6}, psi^{-1}	0.0153
Desorption time, *Days*	0.0148
Fracture compressibility, 10^{-6}, psi^{-1}	0.0014
Water compressibility, psi^{-1}	0.0008
Matrix permeability, *md*	0.0000
Fracture cleat spacing, *ft*	0.0000
Water density. lb/ft^3	0.0000
Initial water saturation, Matrix	0.0000

APPENDIX C

SIMULATION RESULTS FOR PLACKETT-BURMAN METHOD

Table C.1 - Plackett-Burman simulation design

		Simulation Run													
		1	**2**	**3**	**4**	**5**	**6**	**7**	**8**	**9**	**10**	**11**	**12**	**13**	**14**
Parameter	**F1**	-1	-1	1	1	-1	1	1	-1	1	1	-1	-1	1	1
	F2	-1	1	1	-1	1	-1	-1	-1	-1	1	-1	1	-1	1
	F3	1	1	1	-1	-1	1	-1	1	1	-1	-1	1	1	1
	F4	-1	1	1	-1	1	-1	1	1	1	1	-1	-1	-1	1
	F5	1	1	1	-1	1	1	1	-1	1	-1	-1	-1	-1	-1
	F6	-1	1	-1	1	1	1	-1	-1	1	1	-1	1	1	-1
	F7	-1	-1	-1	-1	1	1	1	1	1	1	-1	1	1	-1
	F8	1	-1	-1	1	1	1	-1	1	-1	1	-1	-1	-1	-1
	F9	1	-1	-1	-1	-1	1	1	-1	-1	1	-1	1	-1	1
	F10	-1	-1	1	-1	-1	-1	1	1	-1	1	-1	-1	1	-1
	F11	-1	1	-1	1	-1	-1	1	-1	-1	-1	-1	1	1	1
	F12	1	-1	1	1	-1	-1	1	1	1	-1	-1	1	-1	-1
	F13	1	1	-1	-1	1	-1	1	1	-1	-1	-1	1	1	-1
	F14	-1	-1	-1	-1	-1	1	-1	1	1	-1	-1	1	-1	1
	F15	1	-1	1	1	1	-1	-1	1	-1	1	-1	1	1	1
	F16	-1	1	1	1	-1	1	-1	1	-1	-1	-1	-1	1	-1
	F17	1	1	-1	-1	-1	-1	-1	-1	1	1	-1	-1	1	-1
	F18	1	-1	-1	1	1	-1	1	-1	1	-1	-1	-1	1	1
	F19	1	-1	1	-1	1	1	-1	-1	-1	-1	-1	-1	1	1
	F20	1	1	1	1	-1	1	1	-1	-1	1	-1	1	-1	-1

Table C.1 - Plackett-Burman simulation design

		Simulation Run										
		15	**16**	**17**	**18**	**19**	**20**	**21**	**22**	**23**	**24**	**25**
Parameter	**F1**	0	-1	-1	1	1	-1	1	-1	1	-1	-1
	F2	0	1	-1	1	1	-1	-1	1	1	-1	1
	F3	0	1	-1	-1	1	-1	-1	-1	-1	1	-1
	F4	0	-1	-1	-1	-1	1	1	1	-1	1	-1
	F5	0	1	1	-1	-1	-1	1	-1	1	-1	1
	F6	0	-1	-1	-1	-1	1	-1	-1	1	1	1
	F7	0	1	1	1	-1	-1	-1	1	-1	-1	-1
	F8	0	1	-1	-1	1	-1	1	1	1	1	-1
	F9	0	1	-1	1	-1	1	1	-1	-1	1	1
	F10	0	1	1	-1	1	1	-1	-1	1	1	1
	F11	0	1	1	-1	-1	-1	1	1	1	1	-1
	F12	0	-1	-1	1	-1	-1	-1	1	1	1	1
	F13	0	-1	-1	1	1	1	1	-1	1	-1	-1
	F14	0	-1	1	-1	1	1	1	1	1	-1	1
	F15	0	-1	1	-1	-1	-1	1	-1	-1	-1	1
	F16	0	1	-1	1	-1	1	1	1	-1	-1	1
	F17	0	-1	1	1	1	-1	1	1	-1	1	1
	F18	0	1	-1	-1	1	1	-1	1	-1	-1	1
	F19	0	-1	1	1	-1	1	-1	1	1	1	-1
	F20	0	-1	1	-1	1	1	-1	1	-1	-1	-1

Table C.2 - Plackett-Burman simulation results

		Simulation Run													
		1	**2**	**3**	**4**	**5**	**6**	**7**	**8**	**9**	**10**	**11**	**12**	**13**	**14**
Parameter	**F1**	6.8	6.8	40	40	6.8	40	40	6.8	40	40	6.8	6.8	40	40
	F2	0.0025	0.04	0.04	0.0025	0.04	0.0025	0.0025	0.0025	0.0025	0.04	0.0025	0.04	0.0025	0.04
	F3	0.3	0.3	0.3	0.0025	0.0025	0.3	0.0025	0.3	0.3	0.0025	0.0025	0.3	0.3	0.3
	F4	0.01	1000	1000	0.01	1000	0.01	1000	1000	1000	1000	0.01	0.01	0.01	1000
	F5	50	50	50	0.1	50	50	50	0.1	50	0.1	0.1	0.1	0.1	0.1
	F6	0.017	0.05	0.017	0.05	0.05	0.05	0.017	0.017	0.05	0.05	0.017	0.05	0.05	0.017
	F7	10	10	10	10	200	200	200	200	200	200	10	200	200	10
	F8	200	10	10	200	200	200	10	200	10	200	10	10	10	10
	F9	62.712	62.4	62.4	62.4	62.4	62.712	62.712	62.4	62.4	62.712	62.4	62.712	62.4	62.712
	F10	2E-06	2E-06	4E-06	2E-06	2E-06	2E-06	4E-06	4E-06	2E-06	4E-06	2E-06	2E-06	4E-06	2E-06
	F11	0.55	0.73	0.55	0.73	0.55	0.55	0.73	0.55	0.55	0.55	0.55	0.73	0.73	0.73
	F12	114	68	114	114	68	68	114	114	114	68	68	114	68	68
	F13	109	109	81	81	109	81	109	109	81	81	81	109	109	81
	F14	0.06	0.06	0.06	0.06	0.06	0.4	0.06	0.4	0.4	0.06	0.06	0.4	0.06	0.4
	F15	0.0032	0.001	0.0032	0.0032	0.0032	0.001	0.001	0.0032	0.001	0.0032	0.001	0.0032	0.0032	0.0032
	F16	5	20	20	20	5	20	5	20	5	5	5	5	20	5
	F17	1422	1422	339	339	339	339	339	339	1422	1422	339	339	1422	339
	F18	1	0.77	0.77	1	1	0.77	1	0.77	1	0.77	0.77	0.77	1	1
	F19	1	0.1	1	0.1	1	1	0.1	0.1	0.1	0.1	0.1	0.1	1	1
	F20	6	6	6	6	0	6	6	0	0	6	0	6	0	0
	Response, *MMscf/acre*	0.78293	3.88125	5.1965	0.07494	0.94484	9.128	2.3255	0.04584	18.2913	3.46163	0.05351	0.02495	0.02914	0.05078

Table C.2 - Plackett-Burman simulation results

		Simulation Run										
		15	**16**	**17**	**18**	**19**	**20**	**21**	**22**	**23**	**24**	**25**
Parameter	**F1**	30	6.8	6.8	40	40	6.8	40	6.8	40	6.8	6.8
	F2	0.005	0.04	0.0025	0.04	0.04	0.0025	0.0025	0.04	0.04	0.0025	0.04
	F3	0.003	0.3	0.0025	0.0025	0.3	0.0025	0.0025	0.0025	0.0025	0.3	0.0025
	F4	0.1	0.01	0.01	0.01	0.01	1000	1000	1000	0.01	1000	0.01
	F5	1	50	50	0.1	0.1	0.1	50	0.1	50	0.1	50
	F6	0.042	0.017	0.017	0.017	0.017	0.05	0.017	0.017	0.05	0.05	0.05
	F7	100	200	200	200	10	10	10	200	10	10	10
	F8	100	200	10	10	200	10	200	200	200	200	10
	F9	62.4	62.712	62.4	62.712	62.4	62.712	62.712	62.4	62.4	62.712	62.712
	F10	3E-06	4E-06	4E-06	2E-06	4E-06	4E-06	2E-06	2E-06	4E-06	4E-06	4E-06
	F11	0.607	0.73	0.73	0.55	0.55	0.55	0.73	0.73	0.73	0.73	0.55
	F12	113	68	68	114	68	68	68	114	114	114	114
	F13	89.5841	81	81	109	109	109	109	81	109	81	81
	F14	0.23	0.06	0.4	0.06	0.4	0.4	0.4	0.4	0.4	0.06	0.4
	F15	0.00138	0.001	0.0032	0.001	0.001	0.001	0.0032	0.001	0.001	0.001	0.0032
	F16	10	20	5	20	5	20	20	20	5	5	20
	F17	1109.54	339	1422	1422	1422	339	1422	1422	339	1422	1422
	F18	0.999	1	0.77	0.77	0.77	1	0.77	1	0.77	0.77	1
	F19	0.592	0.1	1	1	1	1	0.1	1	1	1	0.1
	F20	0	0	6	0	6	6	0	6	0	0	0
	Response, *MMscf/acre*	8.182	0.33366	5.72413	4.78875	2.54463	0.03279	45.9888	0.35569	14.9163	0.54635	6.73713

APPENDIX D

ECONOMIC MODEL CALCULATION RESULTS FOR ONE-FACTOR-AT-A-TIME METHOD

Table D.1- One factor at a time simulation runs design

Simulation Run / Parameter	1	2	3	4	5	6	7
F1	1	0.1	50	1	1	1	1
F2	30	30	30	6.8	40	30	30
F3	0.23	0.23	0.23	0.23	0.23	0.06	0.4

Table D.2 - Monte Carlo simulation result, one factor at a time method

NPV(US $)	Frequency	Relative Frequency	Probability Density Function	Cumulative Distribution Function
(931,970)	0	0	0.000E+00	0.000E+00
(645,245)	6	0.0006	2.098E-09	3.008E-04
(358,520)	15	0.0015	5.246E-09	1.354E-03
(71,795)	46	0.0046	1.609E-08	4.412E-03
214,930	76	0.0076	2.658E-08	1.053E-02
501,655	107	0.0107	3.742E-08	1.970E-02
788,380	209	0.0209	7.309E-08	3.555E-02
1,075,105	217	0.0217	7.589E-08	5.690E-02
1,361,830	243	0.0243	8.498E-08	7.997E-02
1,648,555	338	0.0338	1.182E-07	1.091E-01
1,935,281	410	0.041	1.434E-07	1.466E-01
2,222,006	517	0.0517	1.808E-07	1.931E-01
2,508,731	761	0.0761	2.661E-07	2.571E-01
2,795,456	1112	0.1112	3.889E-07	3.510E-01
3,082,181	1467	0.1467	5.130E-07	4.803E-01
3,368,906	1696	0.1696	5.931E-07	6.389E-01
3,655,631	1492	0.1492	5.218E-07	7.988E-01
3,942,356	905	0.0905	3.165E-07	9.189E-01
4,229,081	329	0.0329	1.151E-07	9.808E-01
4,515,806	54	0.0054	1.888E-08	1.000E+00

APPENDIX E

ECONOMIC MODEL CALCULATION RESULTS FOR BOX BEHNKEN METHOD

Table E.1 - Box Behnken simulation design

Simulation Runs / Parameter	1	2	3	4	5	6	7	8
F1	0	1	0	-1	-1	-1	0	1
F2	1	0	-1	0	0	-1	0	0
F3	-1	-1	-1	1	-1	0	0	1
Simulation Runs / Parameter	**9**	**10**	**11**	**12**	**13**	**14**	**15**	**16**
F1	-1	0	0	0	0	1	0	1
F2	1	0	1	-1	0	-1	0	1
F3	0	0	1	1	0	0	0	0

Table E.2 - Box Behnken simulation data

Simulation Runs / Parameter	1	2	3	4	5	6	7	8
F1	1	50	1	0.1	0.1	0.1	1	50
F2	40	30	6.8	30	30	6.8	30	30
F3	0.06	0.06	0.06	0.4	0.06	0.23	0.23	0.4
Simulation Runs / Parameter	**9**	**10**	**11**	**12**	**13**	**14**	**15**	**16**
F1	1	50	1	0.1	0.1	0.1	1	50
F2	40	30	6.8	30	30	6.8	30	30
F3	0.06	0.06	0.06	0.4	0.06	0.23	0.23	0.4

Table E.3 - Monte Carlo simulation result, Box Behnken method

NPV(US $)	Frequency	Relative Frequency	Probability Density Function	Cumulative Distribution Function
(5,086,248)	1	0.0001	1.586E-10	0.000E+00
(4,455,546)	12	0.0012	1.903E-09	6.503E-04
(3,824,844)	31	0.0031	4.917E-09	2.801E-03
(3,194,142)	85	0.0085	1.348E-08	8.604E-03
(2,563,439)	139	0.0139	2.205E-08	1.981E-02
(1,932,737)	232	0.0232	3.680E-08	3.837E-02
(1,302,035)	348	0.0348	5.520E-08	6.738E-02
(671,333)	517	0.0517	8.201E-08	1.106E-01
(40,631)	687	0.0687	1.090E-07	1.709E-01
590,071	960	0.096	1.523E-07	2.533E-01
1,220,774	1149	0.1149	1.823E-07	3.588E-01
1,851,476	1180	0.118	1.872E-07	4.753E-01
2,482,178	1202	0.1202	1.907E-07	5.944E-01
3,112,880	1071	0.1071	1.699E-07	7.081E-01
3,743,582	959	0.0959	1.521E-07	8.097E-01
4,374,284	725	0.0725	1.150E-07	8.939E-01
5,004,987	419	0.0419	6.646E-08	9.511E-01
5,635,689	219	0.0219	3.474E-08	9.830E-01
6,266,391	56	0.0056	8.883E-09	9.968E-01
6,897,093	8	0.0008	1.269E-09	1.000E+00

APPENDIX F

ECONOMIC MODEL CALCULATION RESULTS FOR WELL SPACING STUDY

Table F.1 - Monte Carlo simulation results, 20 acres well spacing

NPV(US $)	Frequency	Relative Frequency	Probability Density Function	Cumulative Distribution Function
(160,000)	0	0	0.000E+00	0.000E+00
(145,789)	2	0.0002	1.408E-08	1.000E-04
(131,579)	4	0.0004	2.816E-08	4.001E-04
(117,368)	42	0.0042	2.956E-07	2.701E-03
(103,158)	59	0.0059	4.153E-07	7.752E-03
(88,947)	161	0.0161	1.133E-06	1.876E-02
(74,737)	183	0.0183	1.288E-06	3.596E-02
(60,526)	356	0.0356	2.506E-06	6.292E-02
(46,316)	449	0.0449	3.161E-06	1.032E-01
(32,105)	622	0.0622	4.378E-06	1.567E-01
(17,895)	797	0.0797	5.610E-06	2.277E-01
(3,684)	1063	0.1063	7.483E-06	3.207E-01
10,526	1420	0.142	9.996E-06	4.449E-01
24,737	1513	0.1513	1.065E-05	5.916E-01
38,947	1343	0.1343	9.454E-06	7.345E-01
53,158	988	0.0988	6.955E-06	8.511E-01
67,368	645	0.0645	4.540E-06	9.327E-01
81,579	245	0.0245	1.725E-06	9.772E-01
95,789	102	0.0102	7.180E-07	9.946E-01
110,000	6	0.0006	4.223E-08	1.000E+00

Table F.2 - Monte Carlo simulation results, 40 acres well spacing

NPV(US $)	Frequency	Relative Frequency	Probability Density Function	Cumulative Distribution Function
(110,000)	0	0	0.000E+00	0.000E+00
(98,421)	4	0.0004	3.455E-08	2.000E-04
(86,842)	21	0.0021	1.814E-07	1.450E-03
(75,263)	43	0.0043	3.714E-07	4.650E-03
(63,684)	110	0.011	9.500E-07	1.230E-02
(52,105)	206	0.0206	1.779E-06	2.810E-02
(40,526)	335	0.0335	2.893E-06	5.515E-02
(28,947)	435	0.0435	3.757E-06	9.365E-02
(17,368)	617	0.0617	5.329E-06	1.463E-01
(5,789)	818	0.0818	7.065E-06	2.180E-01
5,789	1188	0.1188	1.026E-05	3.183E-01
17,368	1266	0.1266	1.093E-05	4.410E-01
28,947	1339	0.1339	1.156E-05	5.713E-01
40,526	1310	0.131	1.131E-05	7.037E-01
52,105	1021	0.1021	8.818E-06	8.203E-01
63,684	722	0.0722	6.236E-06	9.074E-01
75,263	391	0.0391	3.377E-06	9.631E-01
86,842	147	0.0147	1.270E-06	9.900E-01
98,421	26	0.0026	2.246E-07	9.986E-01
110,000	1	0.0001	8.637E-09	1.000E+00

Table F.3 - Monte Carlo simulation results, 60 acres well spacing

NPV(US $)	Frequency	Relative Frequency	Probability Density Function	Cumulative Distribution Function
(80,000)	0	0	0.000E+00	0.000E+00
(70,526)	4	0.0004	4.222E-08	2.000E-04
(61,053)	36	0.0036	3.800E-07	2.200E-03
(51,579)	85	0.0085	8.973E-07	8.250E-03
(42,105)	122	0.0122	1.288E-06	1.860E-02
(32,632)	234	0.0234	2.470E-06	3.640E-02
(23,158)	324	0.0324	3.420E-06	6.430E-02
(13,684)	504	0.0504	5.320E-06	1.057E-01
(4,211)	702	0.0702	7.410E-06	1.660E-01
5,263	937	0.0937	9.891E-06	2.480E-01
14,737	1159	0.1159	1.223E-05	3.528E-01
24,211	1305	0.1305	1.378E-05	4.760E-01
33,684	1317	0.1317	1.390E-05	6.071E-01
43,158	1215	0.1215	1.283E-05	7.337E-01
52,632	943	0.0943	9.954E-06	8.416E-01
62,105	619	0.0619	6.534E-06	9.197E-01
71,579	344	0.0344	3.631E-06	9.678E-01
81,053	119	0.0119	1.256E-06	9.910E-01
90,526	30	0.003	3.167E-07	9.984E-01
100,000	1	0.0001	1.056E-08	1.000E+00

Table F.4 - Monte Carlo simulation results, 80 acres well spacing

NPV(US $)	Frequency	Relative Frequency	Probability Density Function	Cumulative Distribution Function
(70,000)	0	0	0.000E+00	0.000E+00
(61,579)	1	0.0001	1.188E-08	5.001E-05
(53,158)	17	0.0017	2.019E-07	9.501E-04
(44,737)	56	0.0056	6.651E-07	4.600E-03
(36,316)	119	0.0119	1.413E-06	1.335E-02
(27,895)	218	0.0218	2.589E-06	3.020E-02
(19,474)	309	0.0309	3.670E-06	5.656E-02
(11,053)	483	0.0483	5.736E-06	9.616E-02
(2,632)	652	0.0652	7.743E-06	1.529E-01
5,789	946	0.0946	1.123E-05	2.328E-01
14,211	1126	0.1126	1.337E-05	3.364E-01
22,632	1249	0.1249	1.483E-05	4.552E-01
31,053	1274	0.1274	1.513E-05	5.814E-01
39,474	1227	0.1227	1.457E-05	7.064E-01
47,895	1038	0.1038	1.233E-05	8.197E-01
56,316	712	0.0712	8.456E-06	9.072E-01
64,737	387	0.0387	4.596E-06	9.621E-01
73,158	153	0.0153	1.817E-06	9.891E-01
81,579	31	0.0031	3.682E-07	9.983E-01
90,000	2	0.0002	2.375E-08	1.000E+00

Table F.5 - Monte Carlo simulation results, 160 acres well spacing

NPV(US $)	Frequency	Relative Frequency	Probability Density Function	Cumulative Distribution Function
(29,000)	0	0	0.000E+00	0.000E+00
(23,684)	14	0.0014	2.634E-07	7.001E-04
(18,368)	60	0.006	1.129E-06	4.400E-03
(13,053)	170	0.017	3.198E-06	1.590E-02
(7,737)	285	0.0285	5.362E-06	3.865E-02
(2,421)	444	0.0444	8.353E-06	7.511E-02
2,895	712	0.0712	1.340E-05	1.329E-01
8,211	1003	0.1003	1.887E-05	2.187E-01
13,526	1116	0.1116	2.100E-05	3.246E-01
18,842	1172	0.1172	2.205E-05	4.390E-01
24,158	1120	0.112	2.107E-05	5.537E-01
29,474	1098	0.1098	2.066E-05	6.646E-01
34,789	959	0.0959	1.804E-05	7.674E-01
40,105	732	0.0732	1.377E-05	8.520E-01
45,421	539	0.0539	1.014E-05	9.155E-01
50,737	355	0.0355	6.679E-06	9.602E-01
56,053	145	0.0145	2.728E-06	9.852E-01
61,368	60	0.006	1.129E-06	9.955E-01
66,684	14	0.0014	2.634E-07	9.992E-01
72,000	2	0.0002	3.763E-08	1.000E+00

Table F.6 - Monte Carlo simulation results, 320 acres well spacing

NPV(US $)	Frequency	Relative Frequency	Probability Density Function	Cumulative Distribution Function
(12,000)	0	0	0.000E+00	0.000E+00
(9,474)	16	0.0016	6.334E-07	8.001E-04
(6,947)	69	0.0069	2.732E-06	5.051E-03
(4,421)	210	0.021	8.313E-06	1.900E-02
(1,895)	327	0.0327	1.295E-05	4.585E-02
632	649	0.0649	2.569E-05	9.466E-02
3,158	837	0.0837	3.313E-05	1.690E-01
5,684	1027	0.1027	4.066E-05	2.622E-01
8,211	1081	0.1081	4.279E-05	3.676E-01
10,737	1130	0.113	4.473E-05	4.781E-01
13,263	1111	0.1111	4.398E-05	5.902E-01
15,789	1039	0.1039	4.113E-05	6.977E-01
18,316	862	0.0862	3.412E-05	7.928E-01
20,842	697	0.0697	2.759E-05	8.707E-01
23,368	471	0.0471	1.865E-05	9.291E-01
25,895	277	0.0277	1.097E-05	9.665E-01
28,421	140	0.014	5.542E-06	9.874E-01
30,947	45	0.0045	1.781E-06	9.966E-01
33,474	10	0.001	3.959E-07	9.994E-01
36,000	2	0.0002	7.917E-08	1.000E+00

VITA

Name: Pahala Dominicus Sinurat

Permanent Address: Harold Vance Dept. of Petroleum Engineering
TAMU, College Station TX 77843-3116

Email Address: sinurat.pahala@yahoo.com

Education: M.S., Petroleum Engineering
Texas A&M University
College Station, Texas, 2010

B.S., Petroleum Engineering
Institut Teknologi Bandung
Bandung, Indonesia, 2001